DRY SLIDING WEAR STUDIES ON SINTER-FORGED Fe-Cu-C-xMo ALLOYS

A DISSERTATION

Submitted in partial fulfillment of the

requirements for the award of the degree

Of

MASTER OF TECHNOLOGY

in

METALLURGICAL AND MATERIALS ENGINEERING

by

VIGNESH.S

DEPARTMENT OF METALLURGICAL AND MATERIALS ENGINEERING

INDIAN INSTITUTE OF TECHNOLOGY ROORKEE

ROORKEE – 247 667 (INDIA)

MAY, 2016

INDIAN INSTITUTE OF TECHNOLOGY ROORKEE
ROORKEE

CANDIDATE'S DECLARATION

I hereby certify that the work which is being presented in the thesis, entitled "DRY SLIDING WEAR STUDIES ON SINTER FORGED Fe-Cu-C-xMo ALLOYS" in partial fulfillment of the requirements for the award of the degree of Master of Technology and submitted in the Department of Metallurgical and Materials Engineering, Indian Institute of Technology Roorkee, Roorkee is an authentic record of my own work carried out during the period from July, 2015 to April, 2016 under the supervision of Dr. Vikram V. Dabhade, Associate Professor and Dr. Vivek Pancholi, Associate Professor, Department of Metallurgical and Materials Engineering, Indian Institute of Technology Roorkee, Roorkee.

The matter presented in this thesis has not been submitted by me for the award of any other degree of this or any other institute.

(VIGNESH.S)

This is to certify that the above statement made by the candidate is correct to the best of my knowledge.

(Vikram V. Dabhade)
Supervisor

(Vivek Pancholi)
Co-supervisor

Date:

ABSTRACT

Fe-Cu-C system is the most commonly used ferrous alloy system in ferrous powder industry and finds a wide range of applications in automobile industry due to its superior mechanical properties, sinterability and competitive cost. Molybdenum enhances hardenability by providing solid solution strengthening. So, the mechanical properties of ferrous alloys are improved by addition of molybdenum. In this present investigation, an attempt is to find the effect of molybdenum content and compare the results with plain carbon steel. Fe-2Cu-0.7C with 0, 0.5 and 1.5 percentage of Mo was prepared by using a mixture of Ferro-molybdenum powder, and elemental powders of iron, copper and carbon. The powders are mixed and blended initially in a double cone mixture to yield the alloy powders of Fe-0.7C, Fe-2Cu-0.7C, Fe-2Cu-0.7C-0.5Mo and Fe-2Cu-0.7C-1.5Mo. These alloy powders are sintered at 1150ºC for 30 minutes in a reducing atmosphere of 90% nitrogen and 10% hydrogen gas. The sintered components are hot forged immediately at 1150ºC. Again the components are re-forged twice at the same temperature to reduce the porosity content. The forged components are homogenized at 1250 ºC for 4 hours. In addition, samples are heat treated in normalized and quench tempered condition to study the mechanical properties. Mechanical properties were significantly influenced by the addition of Mo as well as with heat treatment conditions. The microstructural study showed mostly ferrite, pearlite and bainite structure in furnace cooled condition whereas a complex microstructure of tempered martensite was observed in the fast cooling condition. Also, with addition of molybdenum grain refinement was also observed. Also, dry sliding wear behavior in normalized, quench and tempered heat treated conditions was studied. Study of wear behavior delineates a complex mechanism of wear (delamination, abrasion and oxidation) in Fe-2Cu-0.7C-xMo alloy depending of the amount of Mo added as well as on heat treatment conditions.

ACKNOWLEDGEMENTS

I would like to express my heartiest thanks and deepest gratitude to my respected supervisors Dr. Vikram V. Dabhade, Associate Professor and Dr. Vivek Pancholi, Associate Professor, Department of Metallurgical and Materials Engineering (MMED) for their inspiration, expert guidance and indefatigable efforts at every stage of this thesis work. My supervisors spent their precious time and efforts directing the research work. I believe that the things that I learned from them will benefit me over the course of my lifetime.

I am highly grateful to Dr.Anjan Sil, Head, MMED, IIT Roorkee and all faculty members of the department for their help and support throughout the course of my research work. My special thanks are due to Dr. S.K.Nath, Dr. B.V.Manoj Kumar for their ever kind string of help and encouragement. I would like to thank all the technical and administrative staff of MMED for their corporation during the tenure of the work.

Sincere and special thanks to all my seniors and colleagues for their moral support and memorable stay at IIT Roorkee. I enjoyed working with Mr. R. Sunil Kumar, Dr. Sanjay Rathore, Mr. Rajavel Muthaiah, Mr. Suntahravel Muthaiah, Mr. Anirudha Mallakar, Mr. Vikas Verma, Dr. Ashish Selokar, Mr. Brij Kishor, Mr.Neeraj Kumar Prasad, Ms. Mitta Divya, Mr.Vikas Agarwal, Mr. Niranjan Kumar, Ms.Nikita Goel, Mr.Gulshan Kumar Pradan, Mr. Yogendra Pratap Singh, Mr.Supratim Endow in MMED.

I would like to express heartiest gratitude to my parents, Mr. S.Sreenivas and Mrs. S. Sabitha for showering their blessings over me. Also, I would like to thank my brother Mr.S.Soorya for his support.

Above all, I express my sincere thanks to GOD from the core of my heart for giving the strength and patience to accomplish my project work.

Roorkee
Dated:

(VIGNESH.S)

TABLE OF CONTENTS

LIST OF FIGURES

LIST OF TABLES

1. INTRODUCTION

Powder metallurgy is continually and quickly evolving technology embracing most alloy materials, and a wide variety of engineered components. Powder metallurgy is a highly developed method of manufacturing reliable in ferrous and non ferrous parts. By producing parts with a homogeneous structure the powder metallurgy process enables manufacturers to make products that are more consistent and predictable in their behavior across a wide range of applications. In addition, the powder metallurgy process has a high degree of flexibility allowing the orienting of the physical characteristics of a product to suit one's specific property and performance requirements.

The Fe-Cu and Fe-Cu-C alloys have for a long period of time been the predominant system for high strength sintered steels used as a base for forging grades of powder in the powder metallurgy industry. Components manufactured by powder forging process show higher densities and less porosities, and thus improved mechanical properties as compared to press and sintered components. Copper imparts liquid phase sintering and also strengthens the alloy by solid solution strengthening and participation hardens due to reduced solubility of Cu in Fe at lower temperatures. Extensive literature review indicated that both Cu and Mo are attractive candidates for the development of high density powder metallurgy alloys for high strength applications with improved hardenability

Addition of various alloying elements like phosphorous, cobalt, nickel, chromium, molybdenum, manganese etc., in Fe-Cu-C system have been studied for the improvement of properties like hardness, strength, toughness, wear resistance, fatigue, etc. Apart from Cu, Mo is one of the most favorable alloying elements in powder metallurgy steel. Mo is not sensitive to oxygen and influences mechanical properties significantly by solid solution strengthening and improves hardenability of steel. Mo is ferrite stabilizer which provides faster and homogeneous distribution of alloying elements. Due to various technical positive aspects of Mo addition in powder metallurgy steel it finds applications in highly stressed components. Previous works in Fe-Cu-C system with and without alloying elements have studied the components in pressed and sintered condition. In this work, the aim is to study the components in sintered and forged condition.

Many researchers carried out the wear studies on powder metallurgy alloys. Alloys under as-sintered and heat treated conditions is subjected to lower wear due to its resistance to plastic flow and high strength. Also, addition of Mo has promoted greater wear resistance to alloy steels due to the bainitic structure.

This experiment and dissertation is concentrated on formation of Fe-Cu-C alloy system with addition of molybdenum by sinter forging route and to study the dry sliding wear behavior of the alloy system in different conditions of heat treatment. In addition to that different characterization techniques like microstructural characterization, hardness test, tensile test, XRD, SEM analysis etc is also studied.

2. LITERATURE REVIEW

2.1 Powder metallurgy and powder forging

Recently, ferrous alloys manufactured by powder metallurgy have been used extensively in automobile industry. Powder metallurgy offers wide range of advantages like ease in manufacturing complex shapes, greater yield in manufacture, less loss of materials, high dimensional tolerances and economy over other manufacturing processes.

Several factor like compaction pressure, density of compacts, sintering temperature, porosity present in it etc., influence the mechanical properties of products produced by powder metallurgy route. Presence of pores degrades the properties and performance fabricated by powder metallurgy, and makes it unsuitable for heavy duty applications. The pores present in it act as local stress raisers which degrades the strength of the component.

Powder forging defined as a process in which un-sintered or sintered metal performs is formed by application of single or repeated no of blows using a forging press. Powder forging process has led to the development of new powder metallurgy materials with higher densification and lowered porosity levels, thus enhancing the mechanical properties of the components.

2.2 Iron-Copper-Carbon (Fe-Cu-C) system

Fe-Cu-C combines the effect of iron-carbon and iron-copper alloy systems. The most common Fe-Cu-C system uses carbon in the range of 0.5% to 0.8% and copper in the range of 2% to 5%. Copper at 1150ºC melts and forms liquid phase sintering which highly helps in particle bonding. Due to the its distinct advantages like good sinterability, superior mechanical properties and competitive cost, Fe-Cu-C alloys find wider application in powder forged connecting rods, converter turbine sleeve, crank shaft belt drive, valve sheet inserts, clutches adjustment rings, cam shaft pulley, oil pump gear, sintered preform for engine block etc[1].

2.3 Fe-Cu and Fe-Mo System

The Fe-Cu phase diagram is shown in Fig. 1 and it can be seen that, there are three invariant reactions which may involve, namely peritectic reactions at 1484^{o}C and 1094^{o}C, and a eutectoid reaction at 850^{o}C[3]. The products of the eutectoid reaction are ϵ- phase i.e., FCC Cu with small amount of Fe in solution, and ferrite or α- phase which contains a small quantity of Cu in solution.

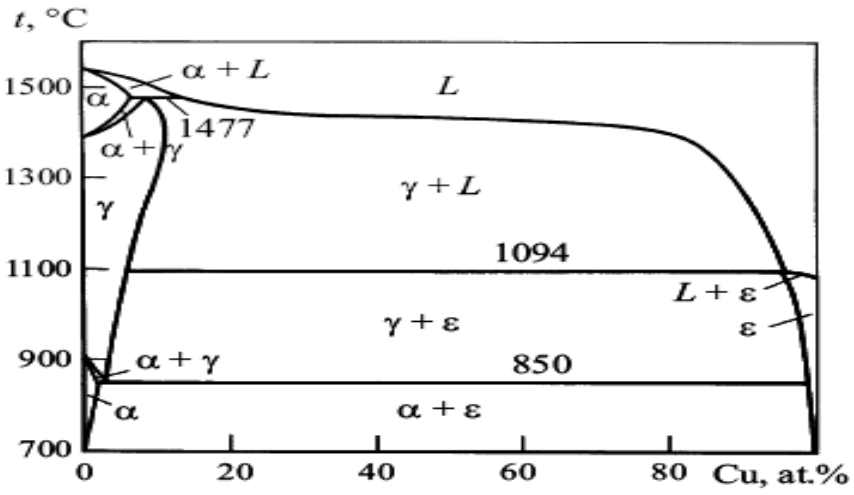

Fig. 1: Fe-Cu phase diagram [2]

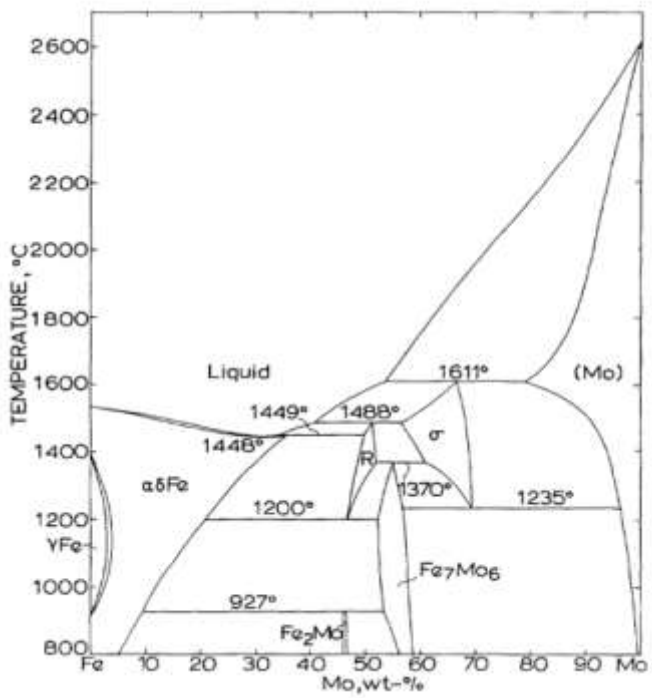

Fig. 2: Fe-Mo phase diagram [2]

A ternary eutectic of iron, copper and carbon exists at a temperature of about 1094°C. Precipitation hardening is possible in Fe-Cu and Fe-Cu-C alloys due to solubility difference of Cu in austenite and ferrite (9wt% in austenite and 0.4wt% in ferrite at room temperature) [12]. When a Fe-Cu alloy with copper content more than 0.4 wt% is heated and cooled rapidly, ferrite supersaturated with copper is formed. Tempering of this supersaturated phase, gives improved hardness and strength due to precipitation of copper particles. The Fe-Cu-C system combines the features of both iron-carbon and iron-copper alloy systems. The most common alloy system uses carbon in the range of 0.5 to 0.8 wt% and copper in the range of 2 to 5 wt% [2]. Melting point of copper is 1083ºC which is below normal sintering temperature employed in Fe-Cu-C alloys (1120°C-1250°C), it exhibits typical liquid phase sintering (LPS). The liquid copper fills the pores of the compact causing densification.

Fe-Mo binary phase diagram is shown in Fig.2. The liquidus falls from the melting point of iron to a minimum at 30 wt% Mo and 1448°C as the molybdenum content is increased. There is an invariant peritectic reaction at 1449ºC at which bcc *αδFe* is formed from liquid and an intermediate phase *R* of composition approximately 49.8 wt% Mo. The maximum solid solubility of iron in molybdenum is 21 wt % Fe at the peritectic temperature of

1611°C. The solid solubility of Mo in Fe falls from 35·7 wt % Mo at 1449°C, the temperature of the L+ $R \rightarrow \alpha\delta Fe$ peritectic reaction, to 21 wt% Mo at 1200°C, where the R-phase decomposes eutectoidally into $\alpha\delta Fe$ and Fe_7Mo_6.[3]

2.4 Effect of alloying elements

2.4.1 Carbon

In ferrous powder metallurgy, pure iron is not used directly for any applications. Some amount of carbon is added to strengthen it. Carbon imparts strength and hardness to steels through the formation of pearlite, bainite and maternsite phase. Pure iron on the contrary has ferrite phase which is softer than pearlite. Strength and hardness for powder Metallurgy steels increase proportionally with increase in carbon content up-to eutectoid composition (0.8% C) in as sintered condition. Beyond the eutectoid composition, there is a formation of iron carbide (Fe_3O) network along the pores and grain boundaries resulting in embrittlement and reduction in impact strength, tensile strength, and elongation [2]. For carbon steels, in hardened and tempered condition, peak value of strength was obtained for 0.65%C. [4, 13]

2.4.2 Copper

Copper was among the first few alloy additions used to enhance strength of the sintered steels. Because of its low melting point (1083°C), Cu is present in liquid phase at conventional sintering temperatures for iron, thus it promotes liquid phase sintering and improves strength of the steel[5, 18]. Copper strengthens and hardens the ferrite phase. Growth of new grains is hindered by copper during re-crystallization after forging increasing strength of sintered steel [9]. With increasing Cu content (0 to 8 % wt) in Fe-0.4C system, ferrite becomes refined and also amount of ferrite decreases with increasing cu content. Copper during liquid phase sintering leads to swelling of the compact and thus making it difficult to maintain dimensional tolerances [2, 11]. Despite of its low melting point, copper does not diffuse fully at conventional sintering temperatures into iron, which results in a gradient of copper from the surface of the compact to the core of it. This effect leads to dimensional growth of the compact after sintering [4]. According to the previous researchers done and dilatometric studies conducted, it is established that the compact swelling caused by copper can be effectively compensated simply by addition of carbon to

the compact. Carbon decreases copper diffusion by changing the wetting angle and dihedral angle of liquid copper on iron [6, 25]. Fig. 3 show dimensional changes in the compact after sintering reduce as amount of carbon increases.

From Fig.3, it can be seen that at 1%wt Cu, the addition of graphite has little effect on dimensional change, where as for 2%wt Cu, carbon decreases dimensional changes. With 1%Cu, enough strengthening cannot be obtained [4], and it is very difficult to control dimension tolerances for higher Cu content (> 2.5%Cu) [7]. So, copper content is fixed as 2 wt%.

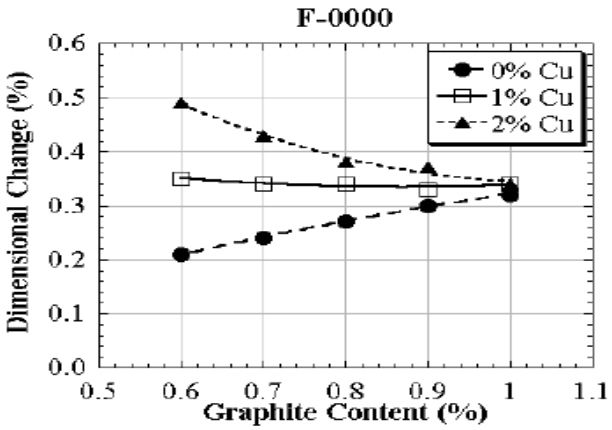

Fig. 3: Dimensional change in Fe-Cu-C for different copper levels [9]

2.4.3 Molybdenum

Addition of an alloying element like molybdenum is very effective which is used in ferrous powder metallurgy industry. It is widely used because it is not oxygen sensitive and has negligible effect on the compressibility of iron powder [3]. Fig. 4 shows the effect of various alloying elements on compressibility of iron powder. It can be seen that Cr and Mo has less effect on compressibility compared to other elements. Molybdenum addition gives solution strengthening effect and also enhances hardenability of steel as it promotes formation of martensitic or bainitic micro-structures through heat treatment. Mo is ferrite stabilizer.

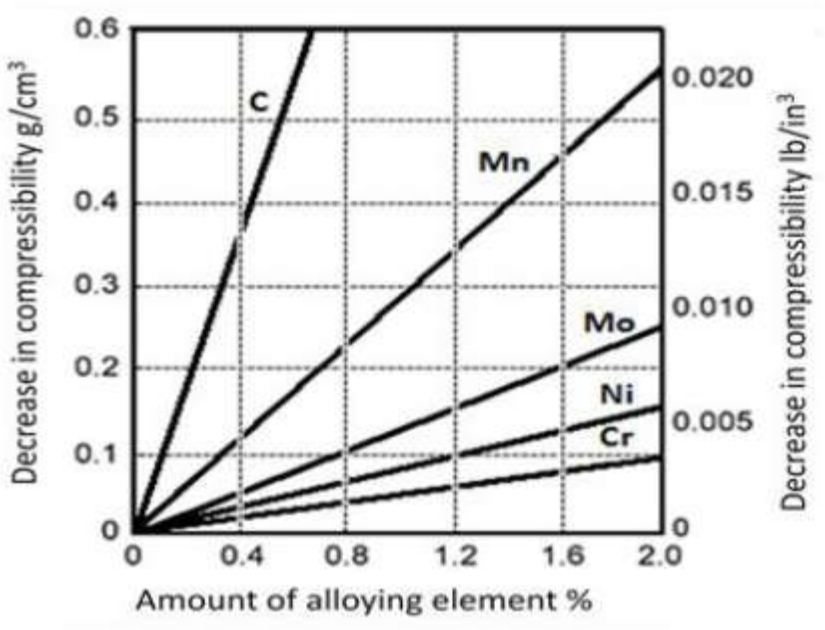

Fig. 4: Effect of Iron powders on compressibility with alloy addition [7]

The addition of Mo and Cu to the base material (Fe-C) was reported to increase tensile strength as well as the hardness of the specimen, but ductility and impact strength was reported to be decrease [3]. The alloy containing Mo was reported to show higher tensile strength compared to the alloy containing Cu or plain carbon steel material [3, 21]. Ferro-molybdenum addition resulted, an improvement in density and micro hardness values of the components. [8]

2.5 Liquid Phase Sintering in Fe-Cu-C:

Sintering is the key step in transforming the green compact to high strength compact. It involves heating of the compact to a temperature where the particles weld to each other.

Sintering in presence of a transient liquid phase which is of interest to the present work is being studied in detail. The commonly used sintering temperature in ferrous powder metallurgy lies between 1100-1300^{o}C. Protective atmospheres are essential to the successful sintering of compacted ferrous metal powders and prevent oxidizing and scale on the surface of the ferrous powder metallurgy parts. Reducing atmospheres are therefore generally used. Vacuum sintering is costly and used only on a small scale in very special cases that essentially require it.

Compact of iron – copper – carbon alloy is considered. Copper in the mixture melts at 1083^{o}C, capillary forces pulls the arising liquid phase into narrow gaps between the particles of the solid component, and contact area between liquid and solid phase is created in the largest possible way. An atmosphere containing 90% H_2 and 10% N_2 (by volume) is produced and sintering is done at a temperature of 1150 ^{o}C (above melting point of copper).

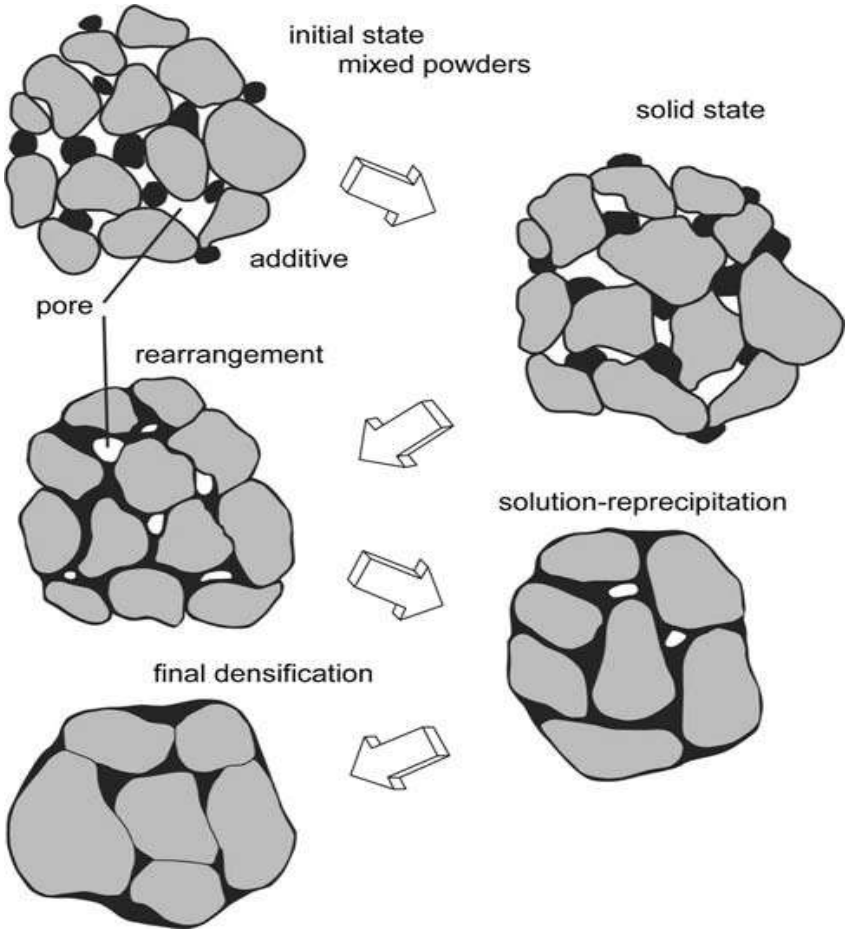

Fig. 5: Different stages of liquid phase sintering [4]

Fig. 5 shows a schematic representation of the microstructure changes during LPS, starting with mixed powders and pores between the particles. During heating the particles sinter, but when a melt forms and spreads the solid grains rearrange. Subsequent densification is accompanied by coarsening. For many products there is pore annihilation as diffusion in the liquid accelerates grain shape changes that facilitate pore removal.

Fig. 6(a), 6(b), 6(c) shows the different stages in sintering of a compact. Left Figure has a solid copper particle and the right Figure shows the pore caused by diffusion of liquid copper into iron. In the similar way when copper diffuses into iron containing graphite, partial disintegration of iron grain boundaries with carbon diffused in it takes place [10]. The latter process requires more work and this can explain the reason of reduced swelling with the addition of graphite.

Fig 6(a) Fig 6(b) Fig 6(c)

Fig. 6: Different stages in sintering of compact [4]

2.6 Density variation with addition of Molybdenum:

Fig.7 shows the variation of green, sintered and as forged density with addition of Mo. With addition of Mo, no significant change was observed in the green and sintered densities. The average green densities were around 69% while that of sintered densities around 72%. Relative forged density of 93-96% is observed in forged compacts due to molybdenum addition.

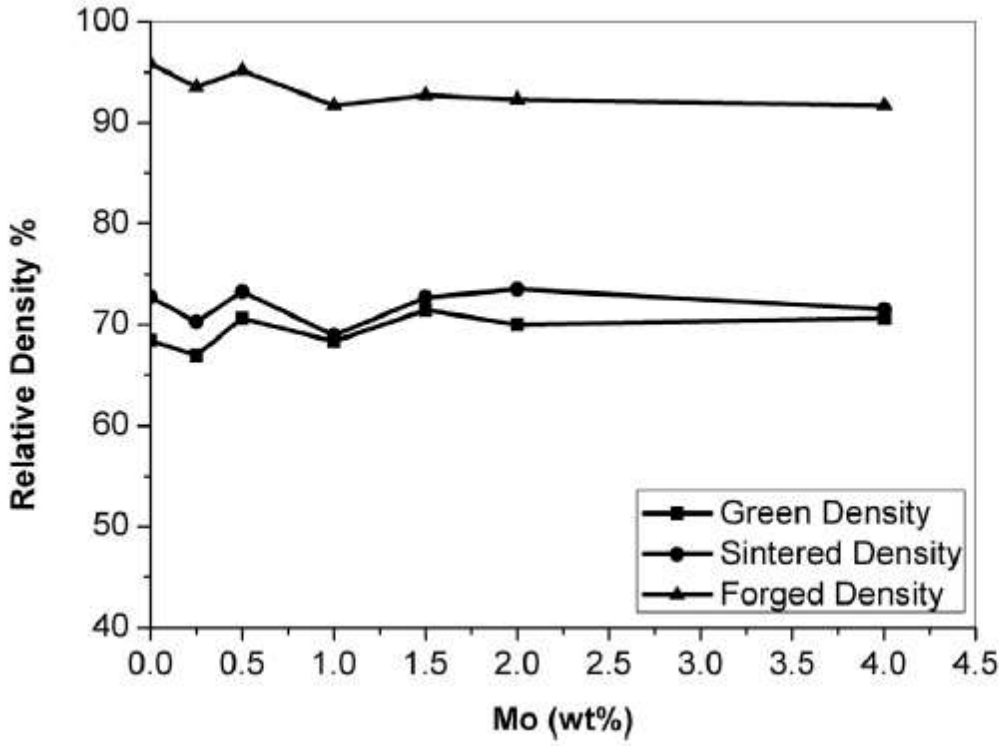

Fig. 7: Effect of Mo addition on the density of Fe-Cu-C system [3]

2.7 Hardness variation of Fe-Cu-C compacts with Mo content:

Fig.8 shows the variation in hardness values under different cooling conditions with addition of Mo content. It is observed that no increase in hardness was observed beyond 1.5 wt% Mo additions. Higher addition of Mo stabilizes ferrite which is a soft phase. Due to corresponding lower compact density, it is observed a dip in hardness values for compacts containing 1 wt% Mo in furnace cooled and water quenched samples.

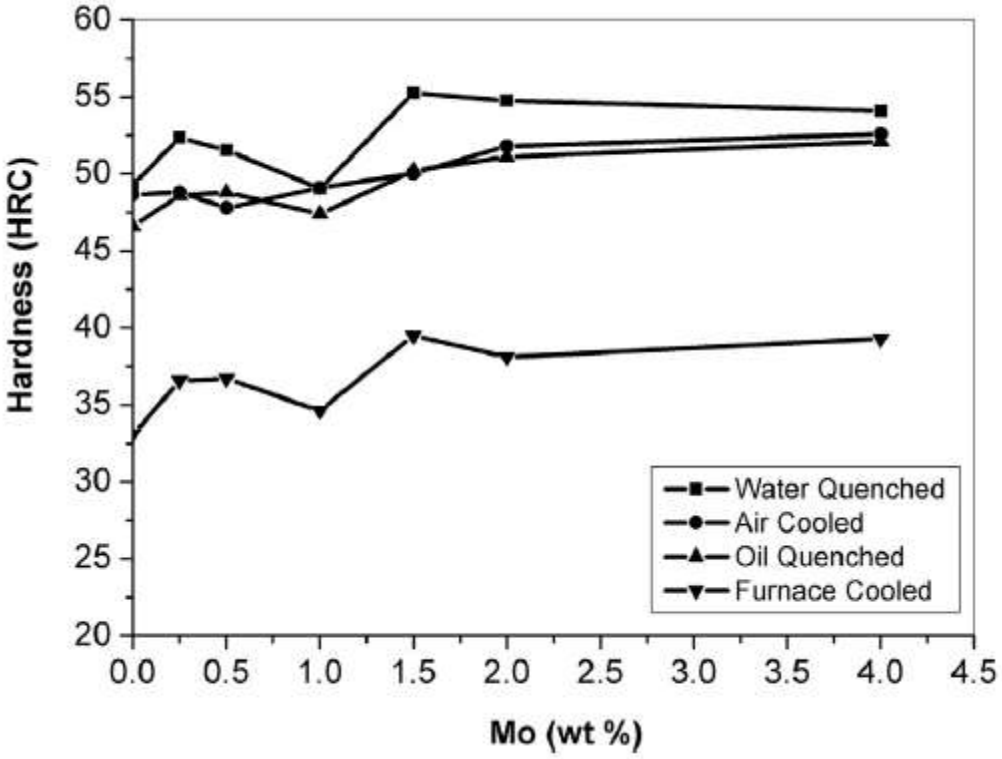

Fig. 8: Variation in hardness of Fe-Cu-C compacts with Mo content with different heat treatment conditions [3]

2.8 Tribological properties of Powder Metallurgy Steels

With growing application of powder metallurgical steels in automobiles, wear and fatigue behavior are major causes of failure in these parts. Wear behavior of steels produced from powder metallurgy are influenced by several factors such as porosity, microstructure, hardness etc, Effect of porosity in wear is peculiar and complex and depends on the wear conditions. In case of lubricated wear, porosity acts as lubricant sink and lubricating channel which is beneficial. In dry sliding wear conditions, both beneficial and detrimental effects of porosity on wear resistance have been reported [8]. Open pores on sliding surfaces collect wear debris generated during sliding and play a positive role as to decrease contact pressure and plastic deformation zone around the pores which decreases wear. On the other hand, presence of pores on the sliding surfaces increases its surface roughness and reduces the load bearing cross section which in turn increases the contact pressure and surface becomes more prone for partial detachment of material during sliding as a result wear of

the surfaces increases. Pore morphology and volume also influence wear behavior of powder metallurgy steels.

Steels exhibit different microstructures when subjected to different rate of cooling which determine the physical and mechanical properties and affect the wear behavior of steels as well. Ferrite which is a soft phase normally is not used for wear resistant applications. Ferrite-pearlite shows comparatively good wear resistance compared to ferrite alone [14, 15]. Superiority of bainitic structure over pearlitic structure for wear resistant applications is a arguable area in steels due to different results obtained in different studies.[8] Wear resistance depends on the transformed microstructures of bainitic steels and when it transformed at low temperature it gives finer, harder and tougher microstructure which exhibits higher wear resistance.[4] Quenched plus tempered heat treatment is widely employed in powder metallurgy steel industry due to tempered martensitic structure compared to highly stressed, hardened martensitic structure obtained from quenched treatment. Hardness of materials is usually employed for predicting their wear behavior. Wear resistance increases with hardness of materials [17]. However, the influence of hardness on wear resistance of powder metallurgical steels is a complex phenomenon as composition; microstructure and wear conditions also alter it. This is also true for sliding wear to a certain extent. This is because there are various sources which cause to vary local hardness such as presence of hard phases like martensite formation, grain refinement, oxidation or plastic deformation etc. and these affect the wear behavior.

3. LITERATURE GAP, PROBLEM FORMULATION AND PLAN OF WORK

3.1 Literature Gap and Problem formulation

1. Mechanical properties of Mo in presence of Cu in Powder metallurgical steel has been investigated earlier, but the wear behavior is yet to be studied.
2. Wear studies of compaction and sintering condition of powders is mostly studied and very scarce data of wear study is available for sinter forged condition.
3. Most of the studies of Mo addition in Fe-Cu-C alloys have been carried out with fully / partially prealloyed powders. Use of elemental powders provides compositional flexibility as well as better compressibility as compared to the prealloyed powders and this route has not been explored fully in the Fe-Cu-C system.
4. The study on effect of Mo addition on mechanical and wear properties in different heat treated condition is also limited.

As the usage of Fe-Cu-C alloys were mainly in automobile application, it is necessary to study the wear behavior of the alloyed steel. As most of the industrial steels are of normalized and quench plus tempered condition, it is important to study the wear behavior of Mo under two different heat treatment conditions.

.

3.2 Plan of work

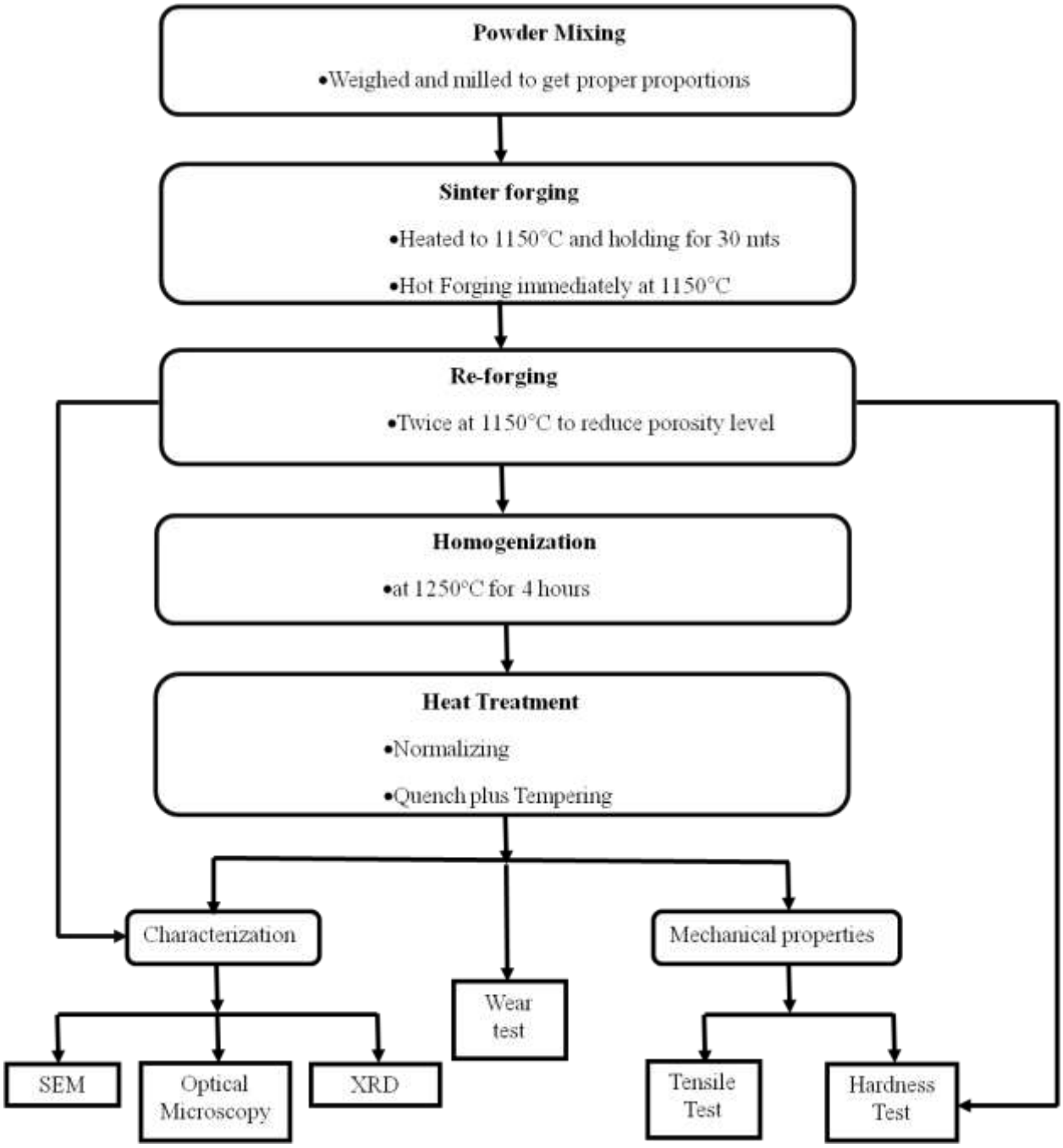

Fig. 9: Schematic representation representing the plan of work

4. EXPERIMENTAL PROCEDURE

4.1. Material Selection:

In current work, elemental iron powder (99.9% purity), carbon in the form of graphite and elemental copper powder (99.7% purity) were used. Molybdenum was added in the form of ferro-molybdenum powder. The chemical composition of ferro-molybdenum powder as given by the supplier is shown in Table 1 below.

Table 1: Composition of ferro-molybdenum powder

Element	Mo	Si	Cu	C	S	P	Fe
Wt %	60	1.5	0.5	0.1	0.08	0.8	Bal.

Four compositions as shown in Table 2 of fixed carbon (0.7 wt %) and copper (2 wt %) content and varying Mo content is investigated in the present study. Composition of Fe-0.7C was also investigated to compare the effect of copper addition.

Table 2 Alloy composition in present study

S No	Composition	Copper (gms)	Carbon (gms)	Ferro-molybdenum (gms)	Iron (gms)	Total wt (gms)
1	Fe-0.7C	0	7	0	993	1000
2	Fe-2Cu-0.7C	20	7	0	973	1000
3	Fe-2Cu-0.7C-0.5Mo	20	7	8.33	964.67	1000
4	Fe-2Cu-0.7C-1.5Mo	20	7	25	948	1000

4.2. Sample preparation:

The steps involved in sample preparation are powder conditioning and mixing, capsule preparation, powder sintering, powder forging, homogenization etc., The details of each step is discussed below:

4.2.1 Powder conditioning and mixing:

Ferro-molybdenum powder (40-50 µm) was wet milled using toluene in a planetary ball mill (Retch PM 400/2 TM) for 2.5 hours at 200rpm to facilitate homogenization by reducing the particle size. Ferro-molybdenum powder is loaded in steel milling jars of 500gm capacity with charge to ball ratio of 1:10. The hardened steel balls of bearing grade of different diameters were used. Earlier investigations revealed that particle size of around 10-15µm was found in 2hr milled samples and average particle size of 4-8µm was found in 2.5hrs milling. So it was decided to mill Fe-Mo powder to 2.5 hrs to ensure a particle size of less than 10µm.

Powders of different compositions shown in Table 2 were weighed carefully in electronic weigh balance and manually mixed in mortar pestle for 30mts and then in double cone mixer for 1.30hrs. Each composition of 1 Kg was prepared and was filled in steel capsule.

4.2.2 Capsule preparation:

A capsule was prepared by joining two hemispherical shape end caps to a hollow pipe by gas welding, whose outer & inner diameters were 63 mm & 61 mm respectively and its length was around 80 mm. Mild steel was the material used to fabricate capsule pipe and end caps. To ensure proper gas passage two stainless tubes were welded at each end. The complete fabricated capsule is shown in Fig. 10 below.

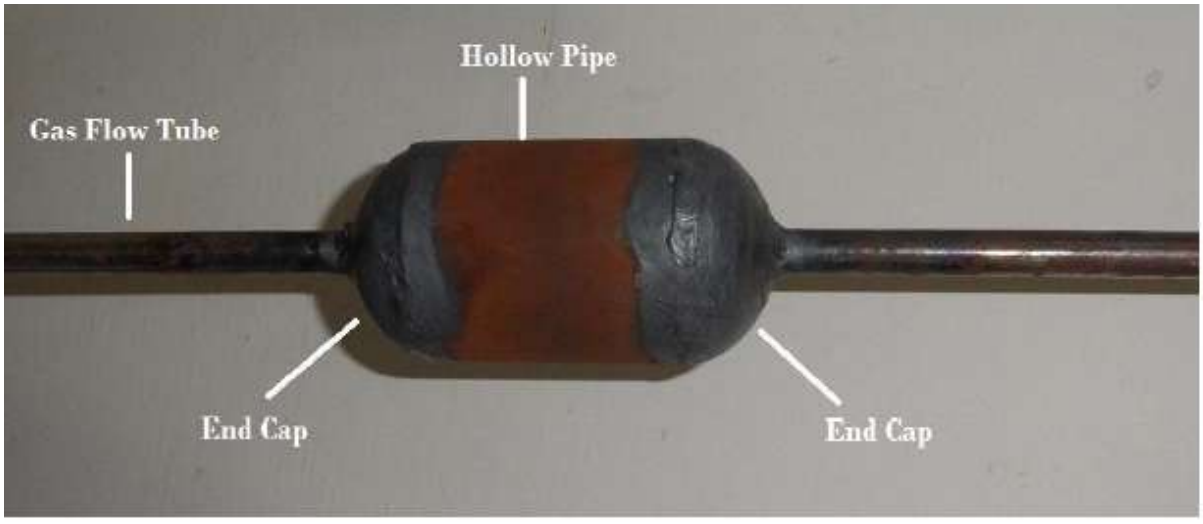

Fig. 10: Completely fabricated capsule

4.2.3 Sintering and forging:

Capsule filled with powders was sintered in a tubular furnace. The maximum operating temperature of the furnace is 1400ºC. The furnace consists of alumina tube of length 3m as shown in Fig. 11.

Fig. 11: Sintering in tubular furnace

Sintering was carried out at 1150ºC with heating rate of 10ºC / min. The capsule was held in the furnace for about 30 min in reducing atmosphere of N_2-10%H_2.

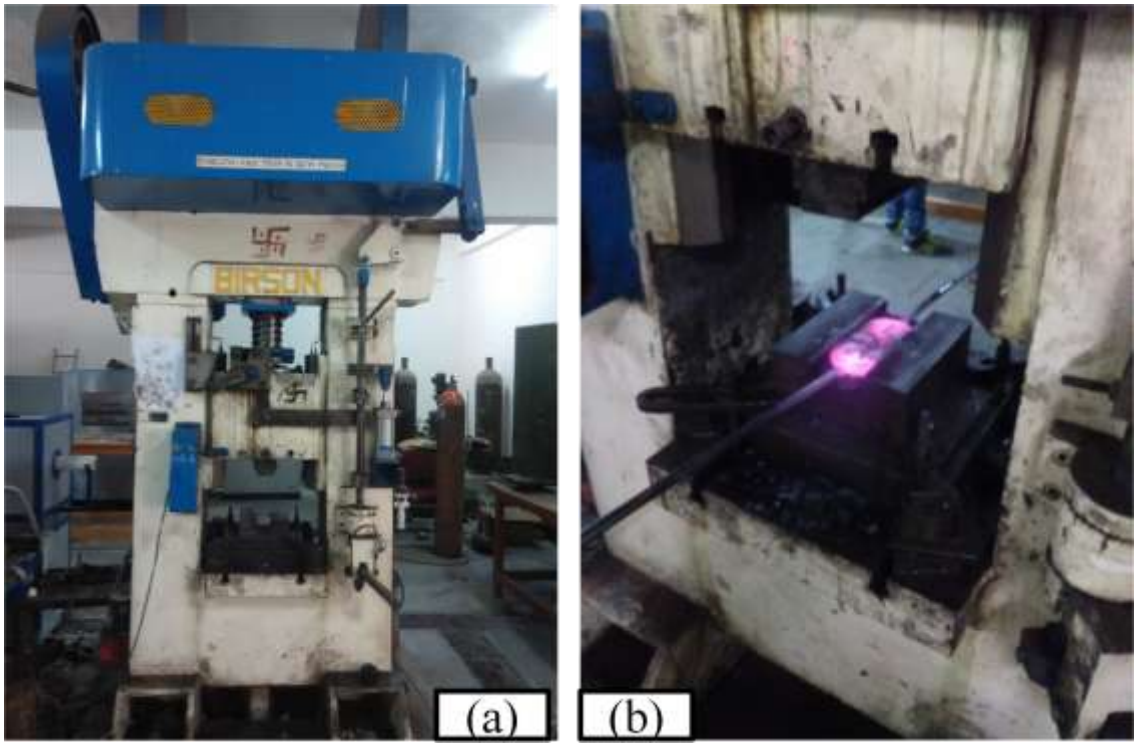

Fig. 12: (a) Friction screw forging press (b) Forged sample in open channel die

The sintered samples were immediately transferred to channel die fitted over a manually operated friction screw press of 100 tonne capacity as shown in Fig. 11 (b). During forging, graphite plus acetone mixture was applied both on the die and punch for lubrication. After forging the slabs were allowed to cool in room temperature. End caps and gas flow tubes were cut-off from the slabs before re-forging. Re-forging is done twice at the same temperature (1150ºC) to reduce the porosity level. Finally rectangular slabs of approximate length: 100-110mm, width: 70-80mm, thickness: 12-14mm was obtained.

4.2.4 Homogenization:

The forged samples were homogenized in a muffle furnace at 1250ºC with heating rate of 10ºC/min and holding time of 4hrs. The samples were coated with graphite plus acetone mixture for reducing the decarburization effect. The homogenization is done inside the furnace as shown in Fig. 13.

Fig. 13: High temperature Muffle furnace

4.2.5 Heat treatments:

Two different heat treatments namely normalizing and quench plus tempering were carried out for all four compositions. Heat treatments were carried out in high temperature muffle furnace at a austenizing temperature of 1050ºC with a constant heat rate of 10ºC/min and holding time of 30min. The plain carbon composition (Fe-0.7C) was heat treated at 950ºC in order to avoid undesired grain growth which was likely to occur at higher temperatures. The normalized samples were taken out from the furnace and air cooled. For quench plus

tempered heat treatment, samples taken out from the furnace were quenched in engine oil at room temperature. The quenched samples were tempered at 350ºC for 1 hour followed by furnace cooling at room temperature. Before loading the samples inside the furnace, the samples were coated with graphite plus acetone mixture for reducing the decarburization effect.

4.3 Mechanical properties testing

4.3.1 Tensile sample preparations and tensile testing:

As per ASTM standard E8M-09, round tensile samples were prepared as per the dimensions shown in Fig. 13 below.

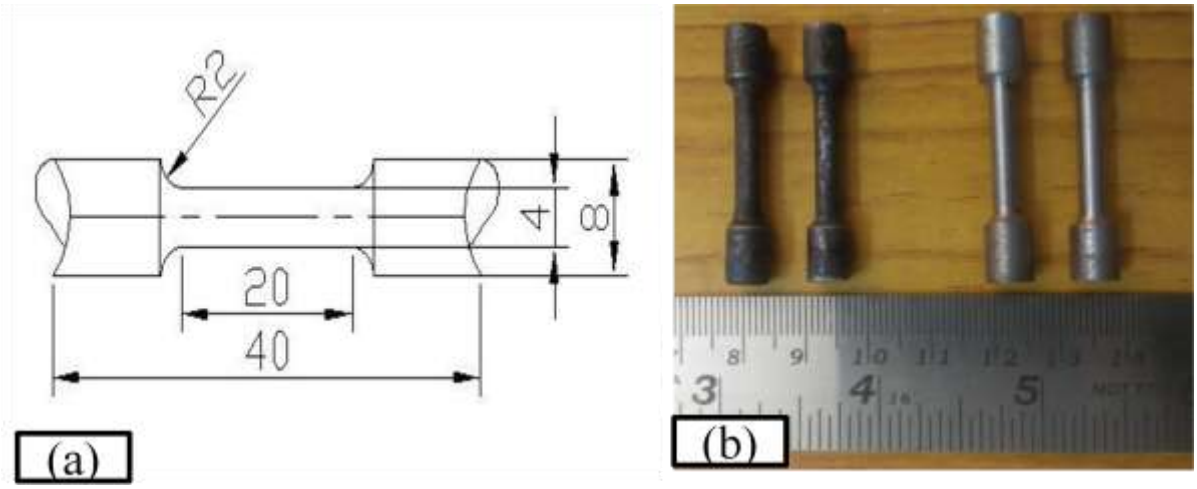

Fig. 13 (a) Schematic diagram of tensile sample (b) tensile sample photograph

Tensile test were carried out for all compositions under both heat treatment conditions at room temperature using H25-S^{TM} (Hounsfield 25KN) computerized tensile testing machine. Load (N) and displacement (mm) logged by the interfaced computer was converted to engineering stress-strain curve for the tested specimen. Two specimens were tested for each composition and heat treatment condition.

4.3.2 Hardness:

There are different definitions for hardness like indentation hardness, rebound hardness, scratch hardness, cutting hardness, abrasive hardness etc., Indentation hardness is resistance offered by the material to indentation by an indenter. Hardness readings are

measured with the help of Vickers hardness testing machine using diamond indenter under 10Kgf load. The Vickers hardness testing machine is as shown in Fig. 14.

Fig. 14: Vickers Hardness testing machine

4.4. Dry sliding wear Test:

4.4.1 Wear test sample preparation:

Wear test specimens (round samples) of dimensions 6mm diameter X 20 mm length were obtained from forged, homogenized and heat treated samples. All samples were polished (both by paper and cloth) to 0.05µm finish. Initial surface roughness was measured by profilometer. Surface roughness and picture of wear samples are shown in Fig. 15.

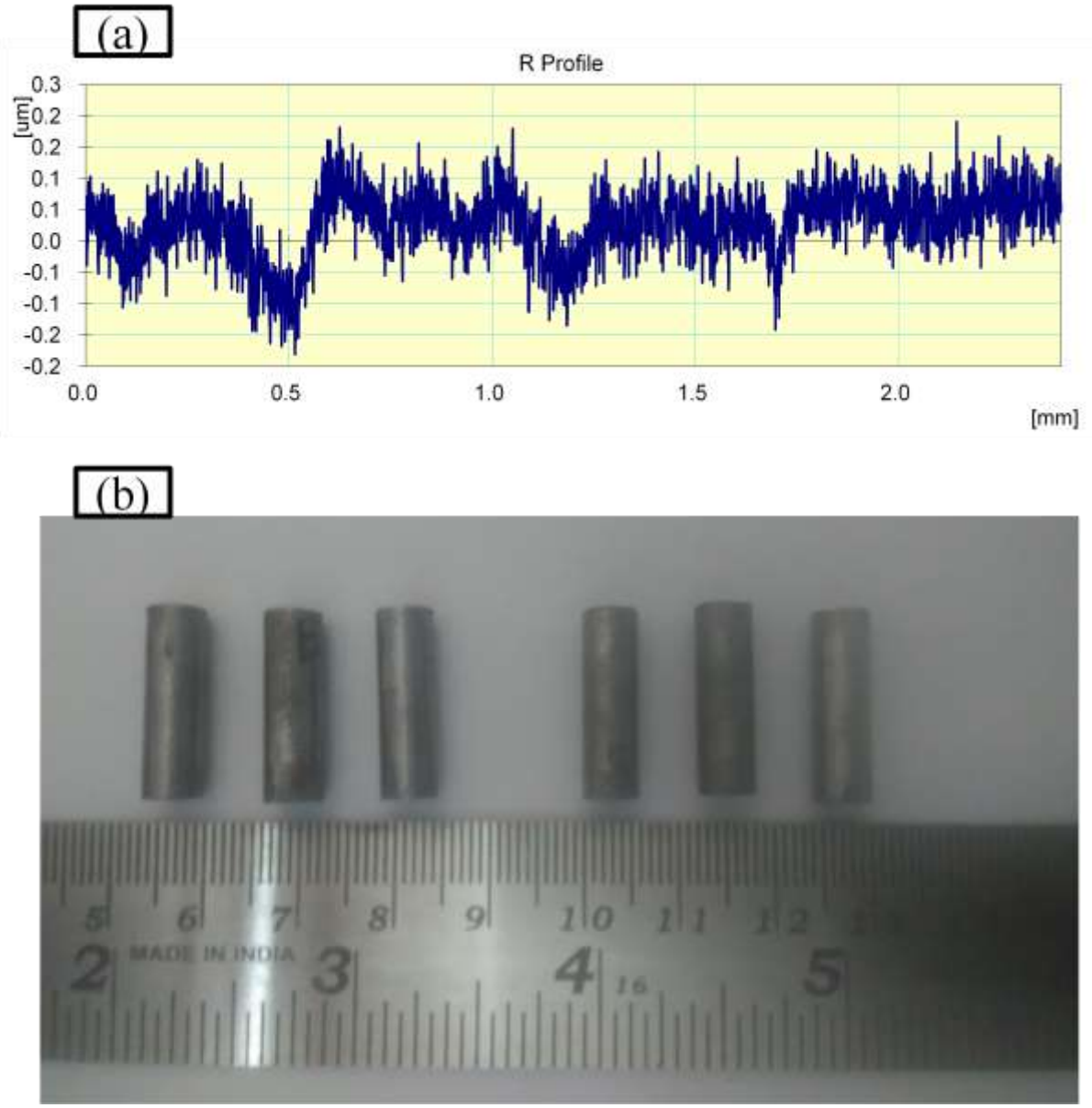

Fig. 15: (a) initial surface roughness of wear specimen (b) Wear specimen used in pin on disc machine.

4.4.2 Wear Test:

Dry sliding wear tests were carried out using pin on disc tribometer TR-201E-M2^{TM} (Ducom, Bangalore, India) as shown in Fig.16. Specifications of tribometer are detailed in Table 3.

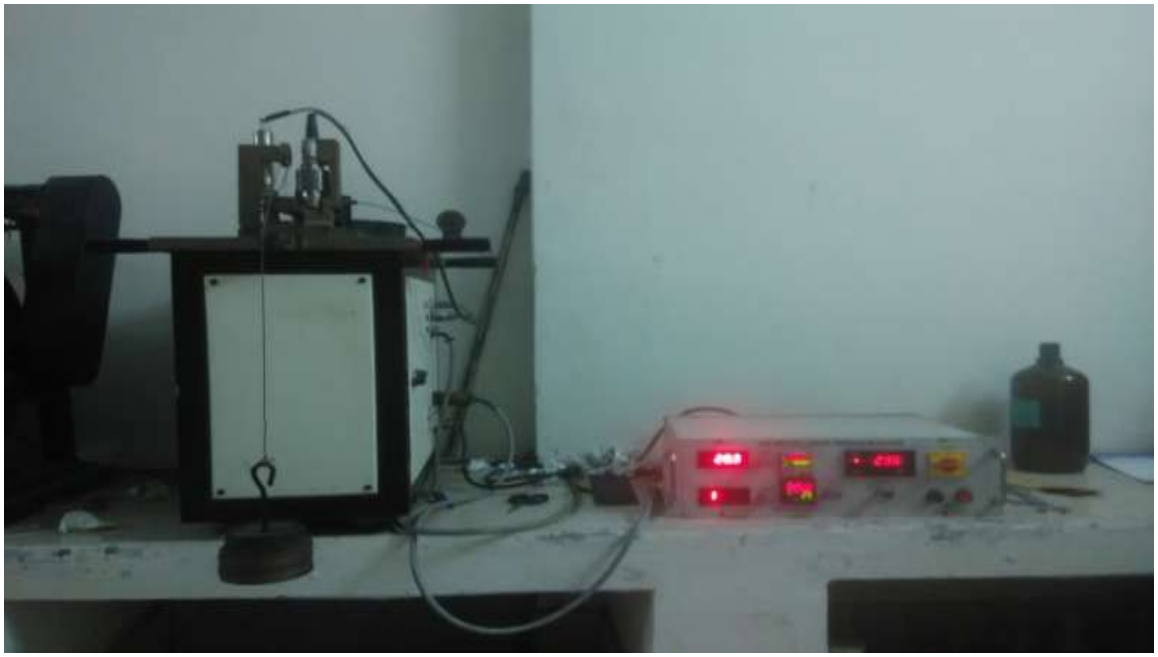

Fig. 16: Pin on disc setup

Friction force was recorded with continuous data logging software, WINDUCOM-2000^{TM} as tribometer was interfaced with the same. Wear tests were conducted at three different loads 20N, 30N and 40N. To determine the effect of sliding speed on wear behavior, wear tests were carried out in 2 sliding speeds of 2m/s and 3.5m/s. All the tests were performed for a fixed sliding distance of 2640m, at room temperature (25^{o}C) and at relative humidity level of 40 ± 5%. Counterface disc has a hardness value of 58HRC. Counter disc was polished after each test and total 2 tests were performed on each condition to obtain the average value.

Table 3: Specifications of Tribometer

Attribute	**Value**
Diameter of wear disc	100mm
Pin diameter	6mm
Pin length	15-30mm
Wear track length	0-80mm
Wear range	2000µm (resolution 1µm)
Disc rotation speed	150-1500rpm
Load	10N-50N (in steps of 5N)
Timer	00/59/59 (hr/min/sec)
Friction force limit	0-50N (resolution 0.1N)

The sliding distance was calculated by position of the ball and the rpm of the disc. The data acquired are the average values taken for three different experiments. The wear rate was calculated by dividing the volume of wear scar by the sliding distance and applied load. The morphologies of worn surfaces of all the samples were studied by using scanning electron microscopy (SEM) to understand the wear mechanism.

4.5 Characterization:

4.5.1 Powder characterization:

The powder morphology was determined under SEM (ZEISS SUPRA 55VP^{TM}) operated in secondary electron imaging mode with 20 kV accelerating voltage. Powder phases were determined by X-ray diffraction (XRD) technique. Both the SEM and XRD analysis techniques have been described in the forthcoming section.

4.5.2 Porosity measurement:

Forged samples are polished by both paper and cloth and then the microstructures were obtained by DMI5000M^{TM} (Leica, Switzerland) metallurgical microscope. The microstructure images are uploaded in Radical Metacheck 5.0 software to obtain the porosity levels.

4.5.3 Microstructural characterization:

Microstructural characterization was carried out using optical microscopy as well as SEM for phase analysis. Microstructural samples of different compositions and heat treatment conditions were sectioned by precision cutting saw, ISOMET 4000^{TM}. Samples were polished on 320, 800, 1200 and 1500 standard grit papers. Again, samples were cloth polished using water suspended polishing alumina grade III to obtain mirror finish. The cloth was rotated at the speed of 150-200rpm mounted on 8" aluminium discs.

4.5.3.1 Optical Microscopy:

Polished surfaces are etched with 2% natal (2ml HNO_3 + 98ml Ethanol) for 10 seconds. The microstructures were observed on LEICA image analyzer having 1000X magnifications with facility of image digitization and capture.

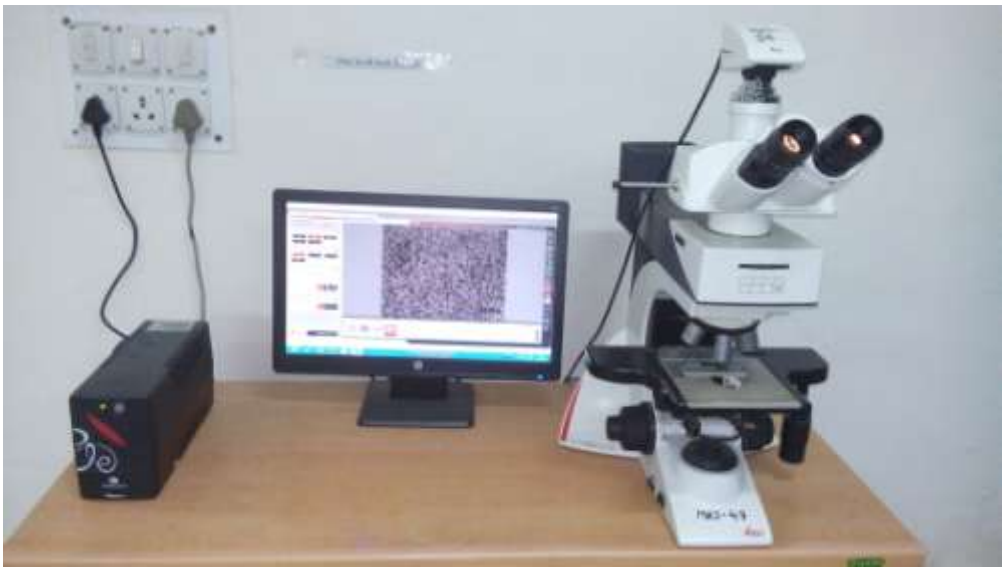

Fig. 17: LEICA optical microscope

4.5.3.2 Scanning electron microscopy (SEM):

Scanning electron microscope (SEM) was employed to observe the morphology of powder samples and also by elemental analysis by the use of EDS (Energy dispersive spectroscopy). The SEM equipment uses an electron beam to scan the sample and the reflected beams of electron is collected and displayed at the same scanning rate on a

cathode ray tube. Magnifications ranging from 10 to an excess of 1.5lakh times is possible with considerable depths of field.

4.5.3.3 X-ray Diffraction (XRD):

XRD is done for phase analysis i.e. to know the phases present in the sample. The sample is bombarded with a X-ray beam generated from cu target, and the diffracted rays are collected at different angles (2Ɵ) to get a plot against intensity against angle of diffraction. From the plots the phases are identified. The specifications of XRD machine are specified below.

Table 4: Specifications of XRD machine

Diffractometer system	XPERT-PRO
Scan type	Continuous
Measurement temperature	27ºC
K-Aplha	1.5406 Å
Generator settings	40mA, 45kV
Anode material	Copper

5. RESULTS AND DISCUSSION

The sintered and forged samples were characterized by using various techniques to study the effect of copper and molybdenum under two heat treated conditions in Fe-2Cu-0.7C-xMo system. The results are discussed below.

5.1 Powder Characterization

The powder samples were characterized by SEM (scanning electron microscopy) to determine the powder morphology and size. The SEM images of ferro-molybdenum powder, iron powder and copper powder are shown in Fig.18 respectively. Ferro-molybdenum powder showed an average particle size of 6 µm. Iron powder was of some irregular shape and average particle size was around 60µm. Copper powder showed dendrite structure with average particle size of 10 µm. Initial particle size of ferro-molybdenum powder was about 45µm. After 2.5 hours of wet milling its size reduced to less than 10µm.

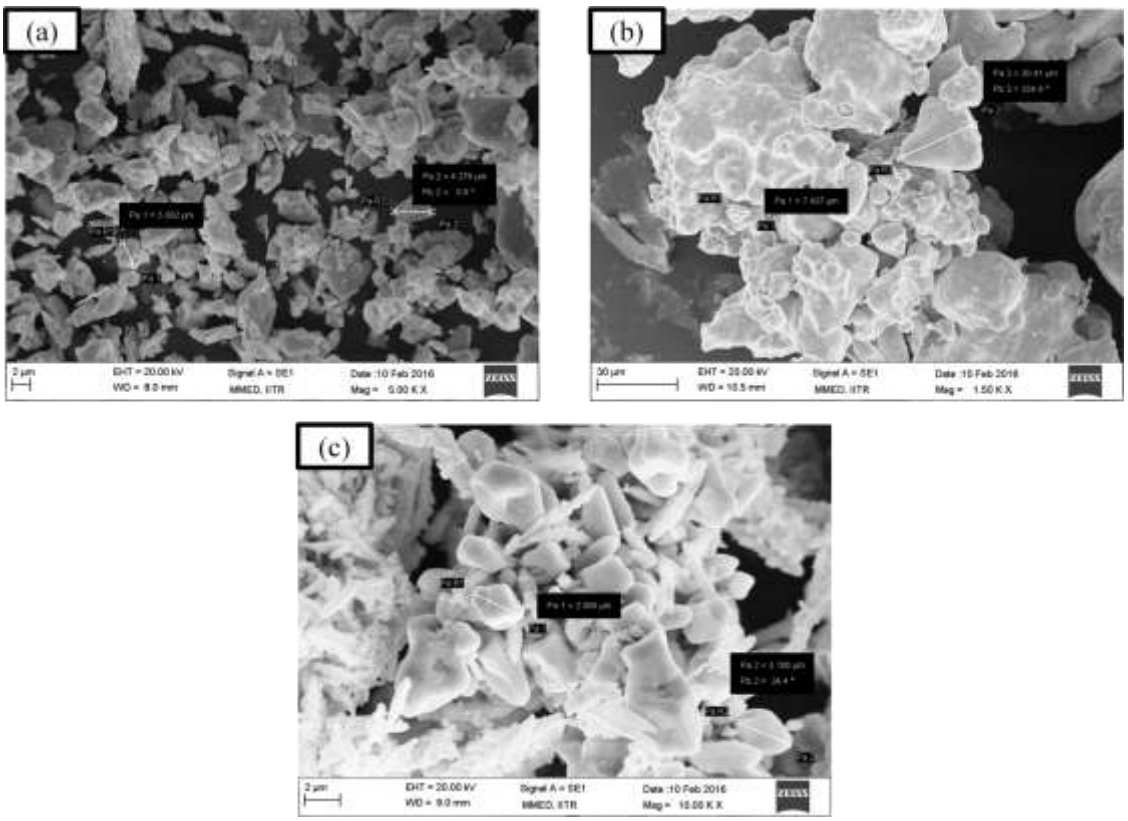

Fig. 18: SEM Images of powder samples (a) Ferro-Molybdenum (b) Iron (c) Copper

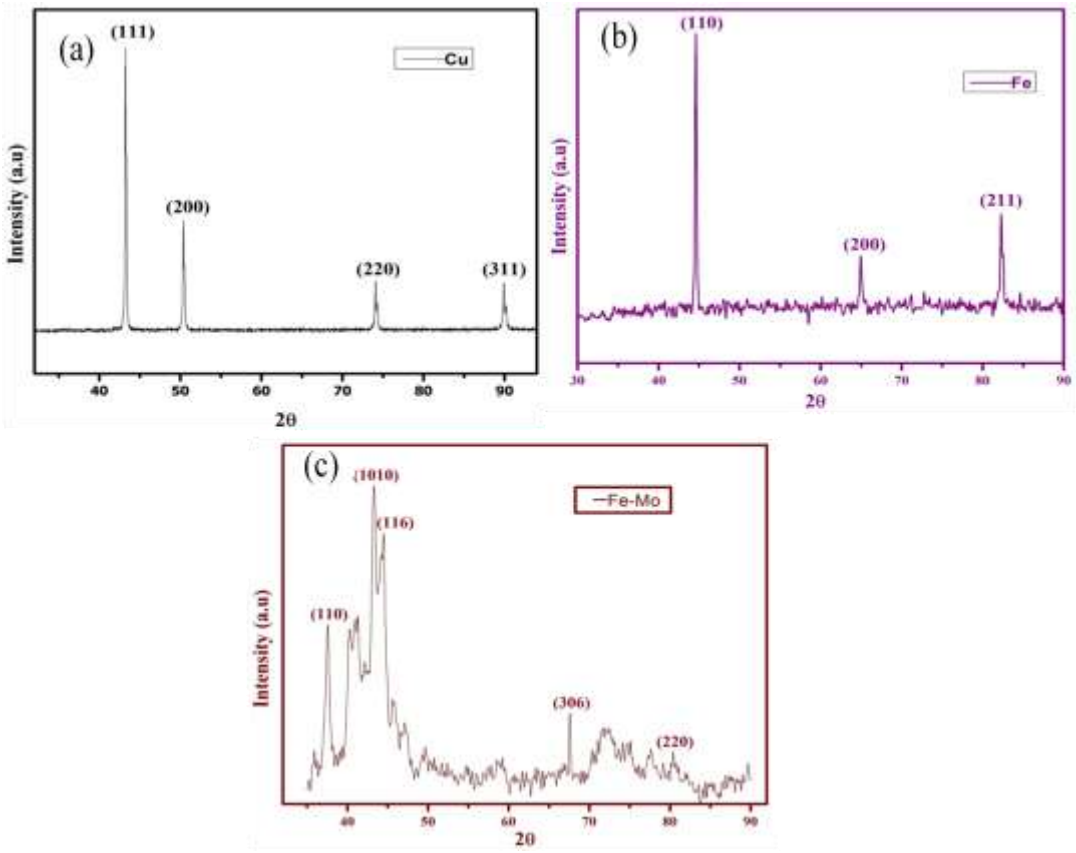

Fig. 19: XRD pattern of powders (a) Cu (b) Fe (c) Fe-Mo

The X-ray diffraction (XRD) pattern of Cu powder, Fe powder and Fe-Mo powder is as shown in Fig.19. As copper has less affinity towards oxygen, it does not oxidize at room temperature. Ferro-molybdenum powder showed all peaks corresponding to Fe_3Mo. The diffraction pattern of Fe powder also exhibited all peaks corresponding to ferrite (bcc).

5.2 Porosity measurement

Polished Samples were observed under optical microscopy for porosity measurement. Porosity was calculated with the help of Radical Metacheck 5.0 software as shown in Fig.20. It can be seen that porosity level gradually decreases after every forging. Addition of copper in plain carbon steel led to less porosity during sinter forging due to liquid phase sintering effect. It can be seen from the graph that the porosity level is less than 2% which indicates a relative density of 98% is obtained.

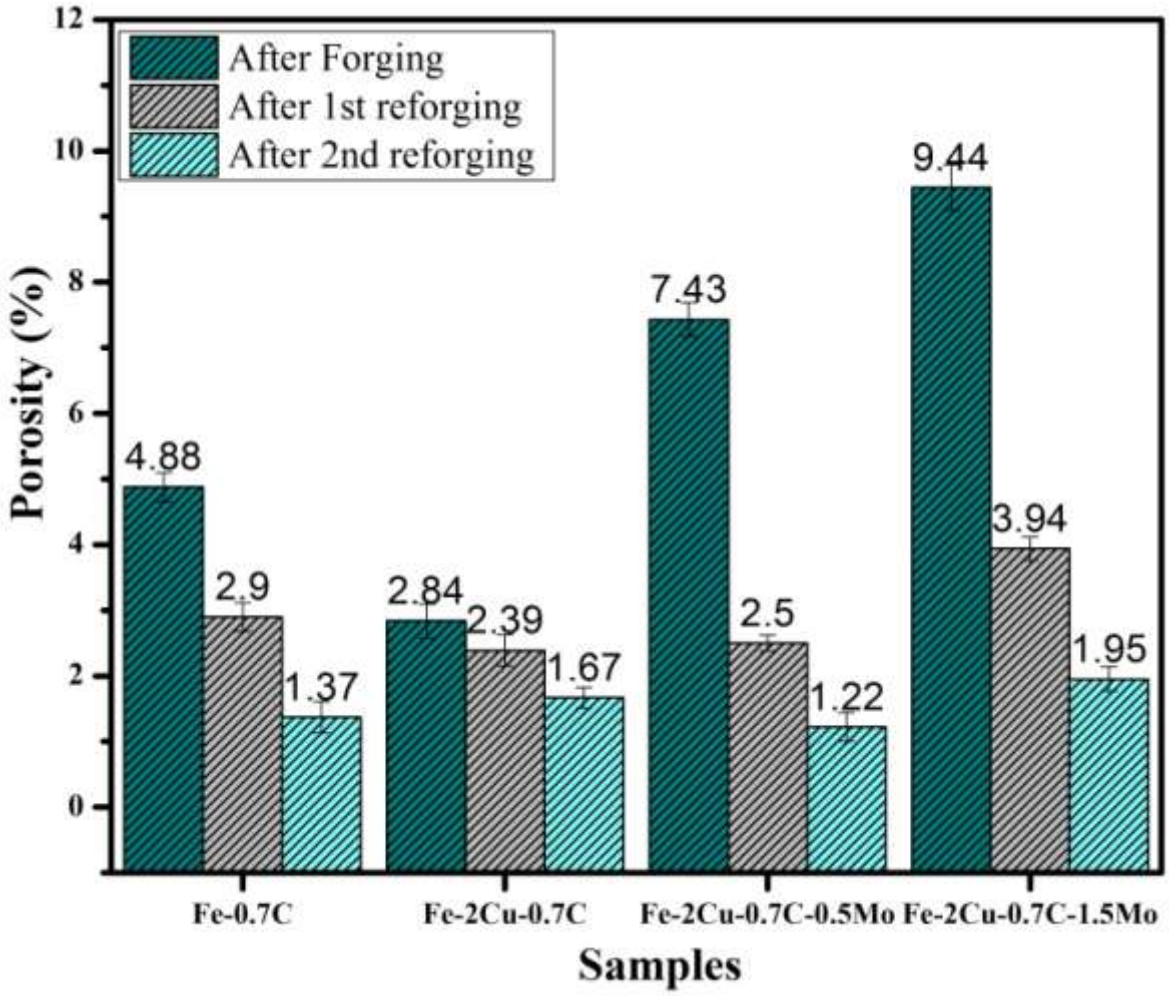

Fig. 20: Variation of porosity with respect to number of forging

It should also be noted that some copper and molybdenum remains undissolved and appears as dark regions in the microstructure. This also adds to the porosity level as the software used to measure the porosity is unable to distinguish between the porosity and the undissolved particles. Thus, the reported density level (>98%) is likely to be even higher though the exact value was difficult to access. Fig.21 (a-c) shows the unetched microscopy images of Fe-2Cu-0.7C-0.5Mo in as-forged, 1st re-forged and 2nd re-forged conditions.

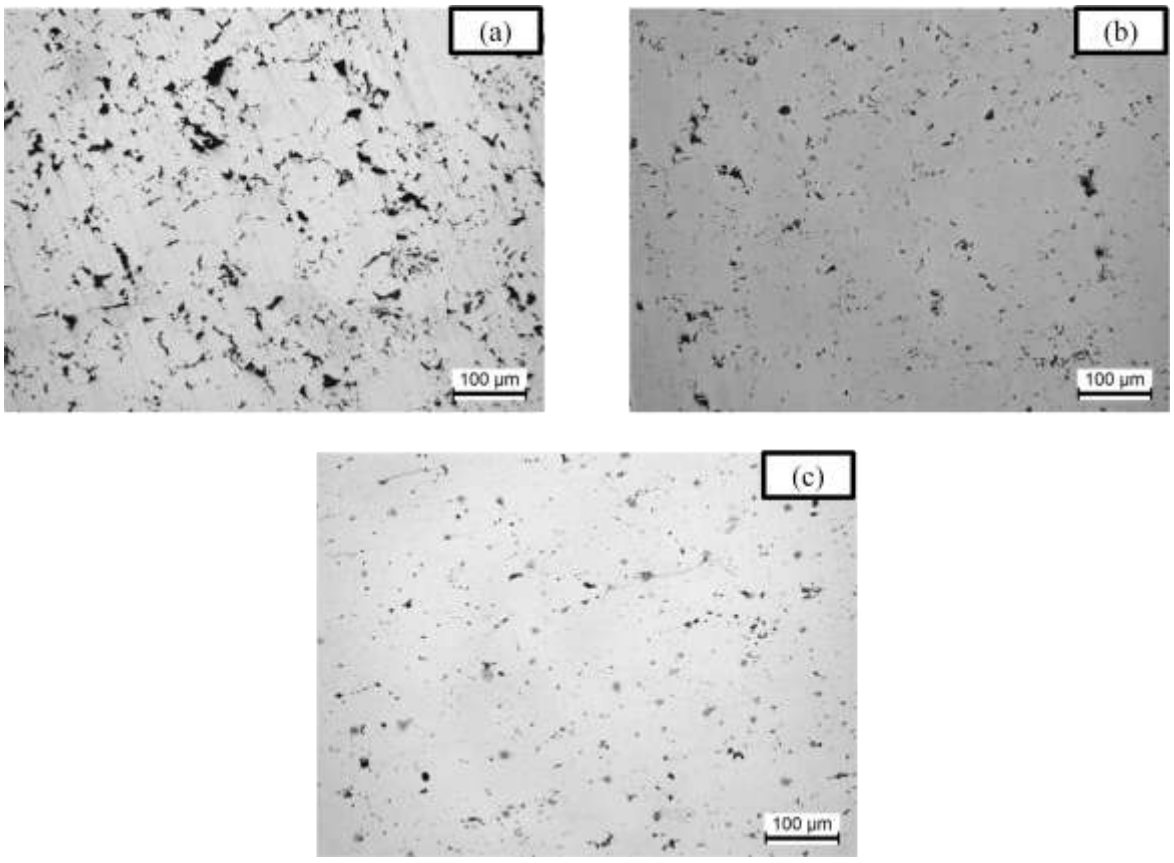

Fig. 21: Unetched micrographs and porosity values of Fe-2Cu-0.7C-0.5Mo sample in (a) as-forged (b) first re-forged (c) second re-forged conditions

5.3 Mechanical Properties

5.3.1 Hardness:

Fig.22 shows the variation of hardness of four different compositions under two different heat treatment conditions. Hardness was found to increase with respect to increase in Mo content. The increase is considerable in normalised condition compared to quench plus tempered condition. Hardness variation can be attributed to microstructural changes that occurred during faster cooling conditions. The normalised microstructures were of ferrite-pearlite / ferrite-bainite which will be discussed in up-coming sections.

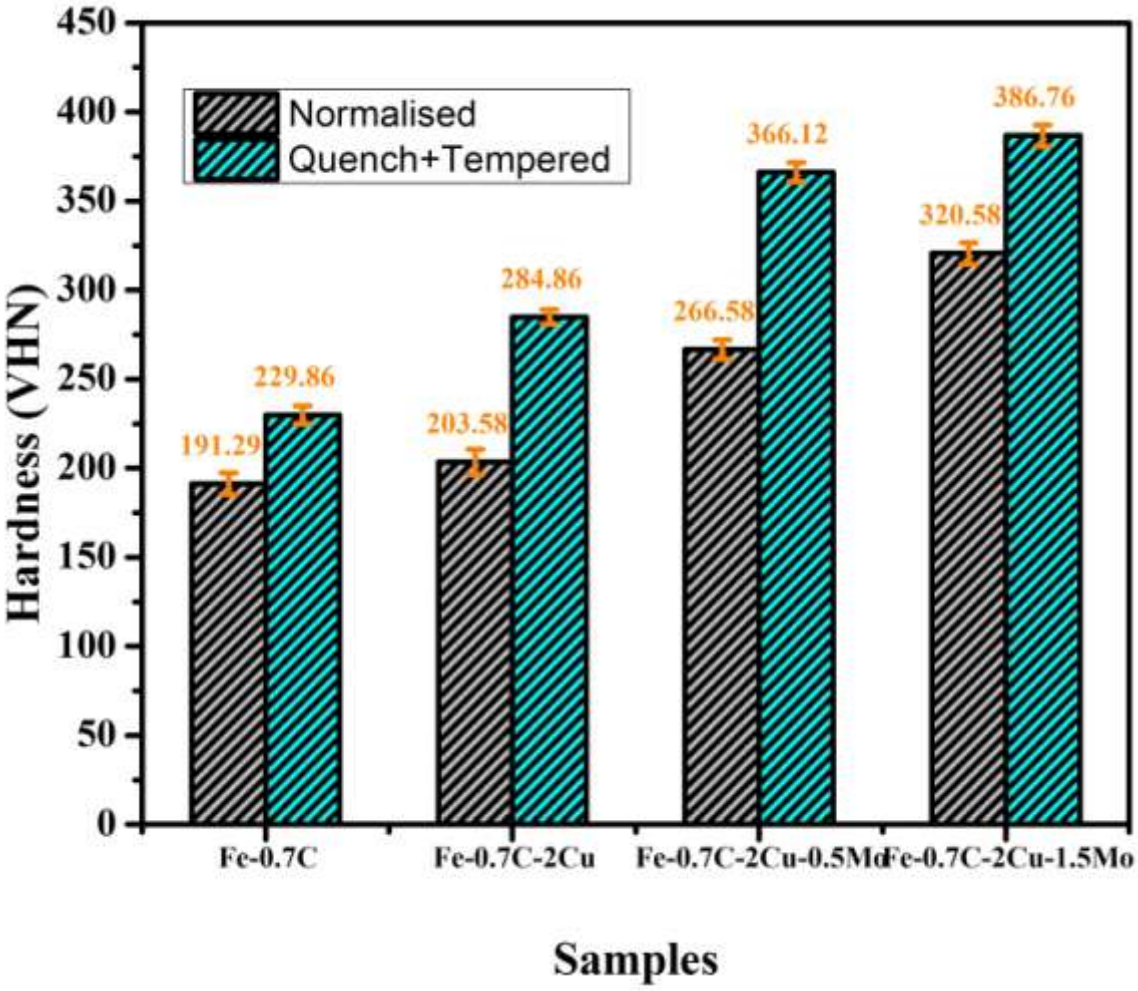

Fig.22: Hardness variation in Fe-0.7C, Fe-2Cu-0.7C, Fe-2Cu-0.7C-0.5Mo, Fe-2Cu-0.7C-1.5Mo under normalised and quench plus tempered conditions.

During quenching, the austenite converts to martensite which causes volume expansion to occur which deforms the surrounding ferrite and increases dislocation density which contributes to increase in hardness [3]. Also, solid solution strengthening effect of Mo in the ferrite contributed for increase in hardness. During tempering softening of martensite takes place and tempered martensite is formed. This change is due to microstructural changes and solid solution effect of carbon. The hardness of Fe-0.7C alloy exhibited around 190 and 230 VHN in normalised and Quench plus tempered condition.

5.3.2 Tensile strength and Elongation:

The tensile behavior of various compositions under two different heat treatments i.e. normalised, and quench plus tempered are shown in Fig.23 as representative stress-strain plots. Alloys containing 0 wt% Cu (Fe-0.7C) and 0 wt% Mo (Fe-2Cu-0.7C) exhibited yield point phenomenon in normalised condition and same had disappeared with addition of Mo in both heat treatment conditions. On the other hand, no yield point was observed in quench plus tempered conditions in any of the compositions investigated.

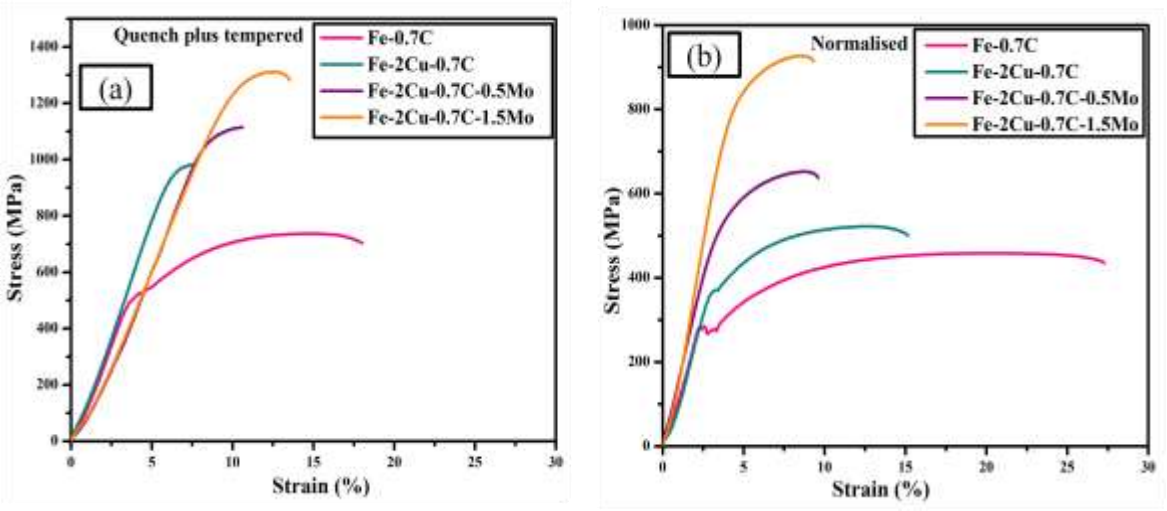

Fig. 23: Representative engineering stress-strain plots of various compositions under (a) Quench plus tempered, (b) Normalised condition respectively.

The variation in tensile strength and ductility for different alloys under two different heat treatment conditions is shown in Fig.24 below. Tensile strength is greatly influenced by addition of alloying elements as well as heat treatment conditions. Addition of molybdenum exhibited considerable increase in strength. It occurs due to solid solution strengthening of Mo. Higher Mo addition stabilizes ferrite phase and restricts gamma loop. Since Mo is strong carbide former and therefore, addition of Mo is likely to form more amount of carbides that would also contribute to increase in strength.

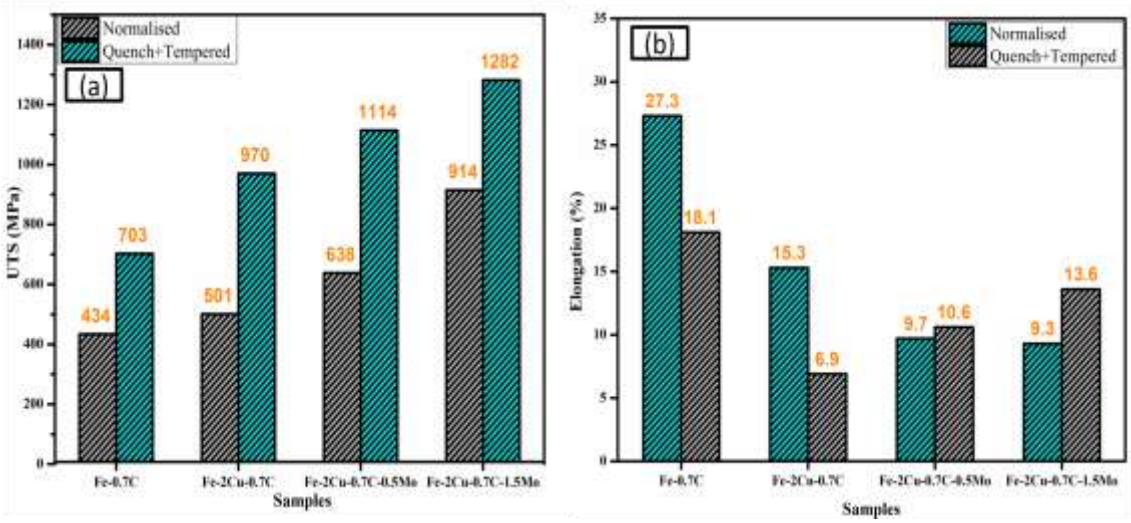

Fig. 24: Represents (a) UTS, (b) Ductility of different alloys under two heat treatment conditions

In quench plus tempered condition ductility was observed to increase with addition of Mo. This is due to the effect of stabilization of ferrite as Mo is ferrite stabilizer. During quench plus tempering, the dispersion of phases or structures takes place in the microstructure which results in improvement of properties [19]. During tempering, relieving of stresses set up during quenching and reduction of brittleness of martensite. Also, transformation into tempered martensite improves the strength values as compared to those in the quench condition. Strength was found to increase with severity of quench, indicating the strengthening effect of Cu & C in the Fe-Cu-C alloy. Carbon is likely to be in the form Fe_3C in the pearlite structure while some carbon will form an interstitial solid solution in ferrite. In quench plus tempered conditions Cu is likely to be in the solid solution of ferrite whereas C is in the BCT lattice of martensite.

5.4 Microstructures:

Fig.25 shows normalized microstructures of different alloy system respectively. Both Cu and Mo increase the hardenability of steel and shift the CCT curves to the right which in turn decreases the chances of pearlite formation and increases the possibility of formation of harder phases like bainite and martensite [20]. Effect of Mo addition on hardenability is more marked than Cu addition [20]. Therefore, increase of Mo addition resulted in bainitic in normal cooling condition and martensitic structures in the faster cooling conditions.

Bainitic region gets progressively increased with increasing Mo content as Mo addition promotes bainite formation and suppresses pearlite formation which is clearly visible in the microstructures. SEM images as in Fig.26 shows clearly the bainite structure due to addition of Mo in normalised condition.

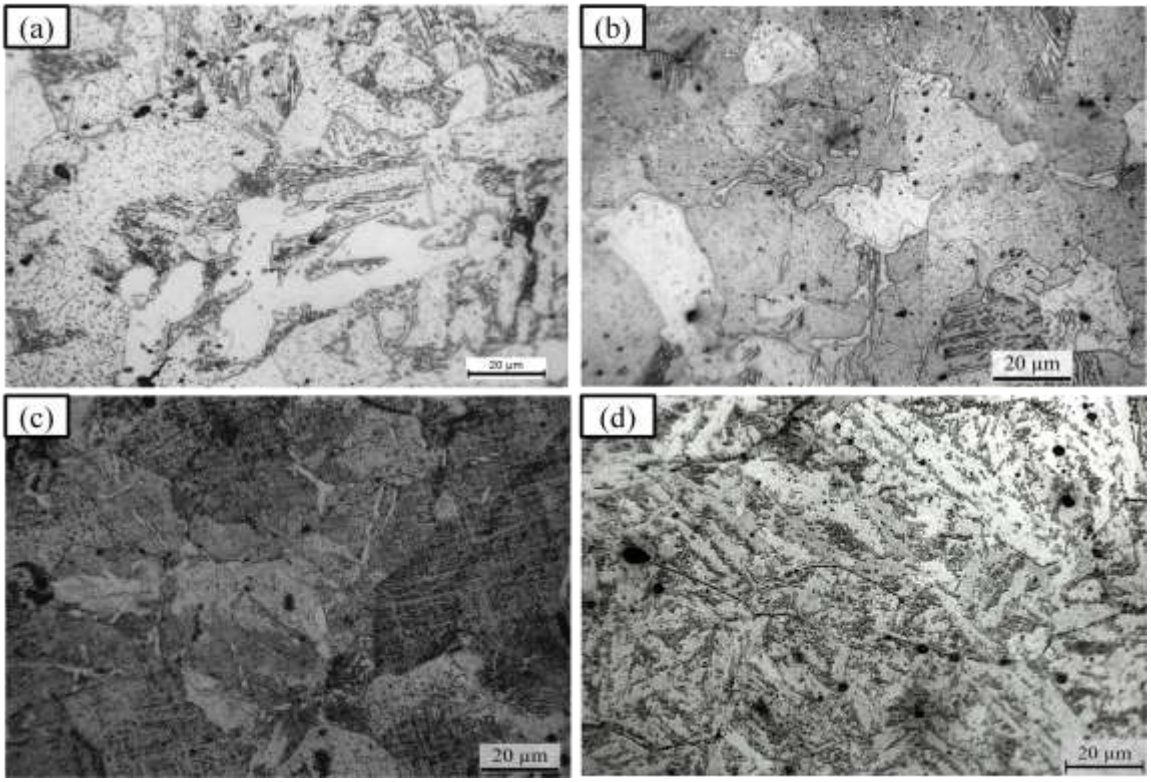

Fig. 25: Micro structures of (a) Fe-0.7C (b) Fe-2Cu-0.7C (c) Fe-2Cu-0.7C-0.5Mo (d) Fe-2Cu-0.7C-1.5Mo in normalised condition

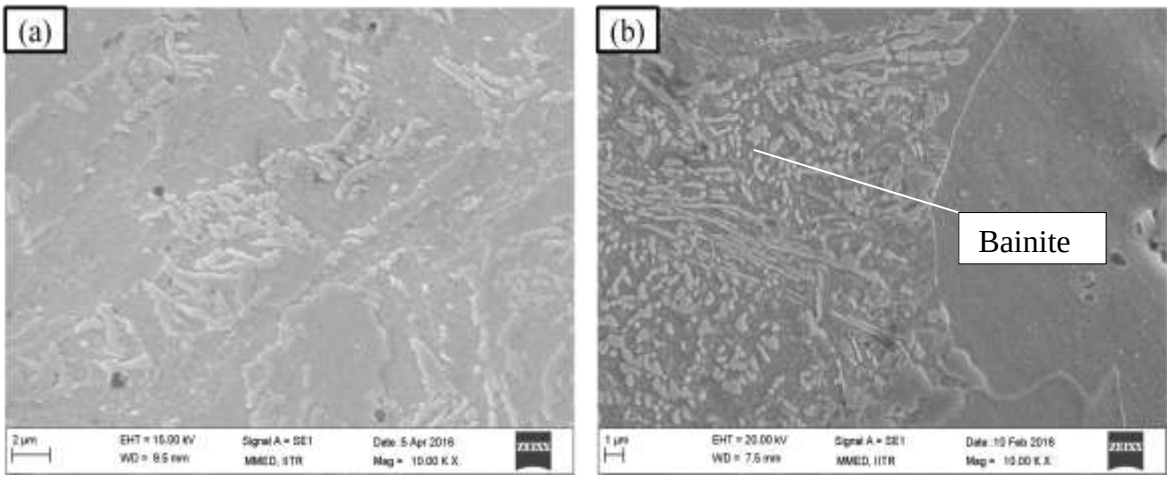

Fig. 26: SEM images of ferrite-bainite in (a) Fe-2Cu-0.7C-0.5Mo (b) Fe-2Cu-0.7C-1.5Mo

Fig.27 shows the microstructures of different alloy system in quench plus tempered condition. Tempered martensite is primarily seen in all the microstructures. During tempering, the martensite present in it gets soften to become tempered martensite.

During quenching, the formation of martensite occurs, which is a very hard phase. But during tempering at 350ºC the martensite converts to complex structure. During tempering the tetragonal martensite changed to a heterogeneous mixture of ferrite and highly dispersed iron carbides which soften the hard martensite. As per the literature the complex structure must be tempered martensite.[3] During the tempering at 350ºC Mo carbides did not form because below the temperature range 500-600°C Mo cannot diffuse rapidly to allow Mo carbides to nucleate. As Mo remained in substitutional solid solution therefore, high tempering temperatures are needed for the necessary diffusion of Mo prior to the nucleation and growth of the Mo carbides.

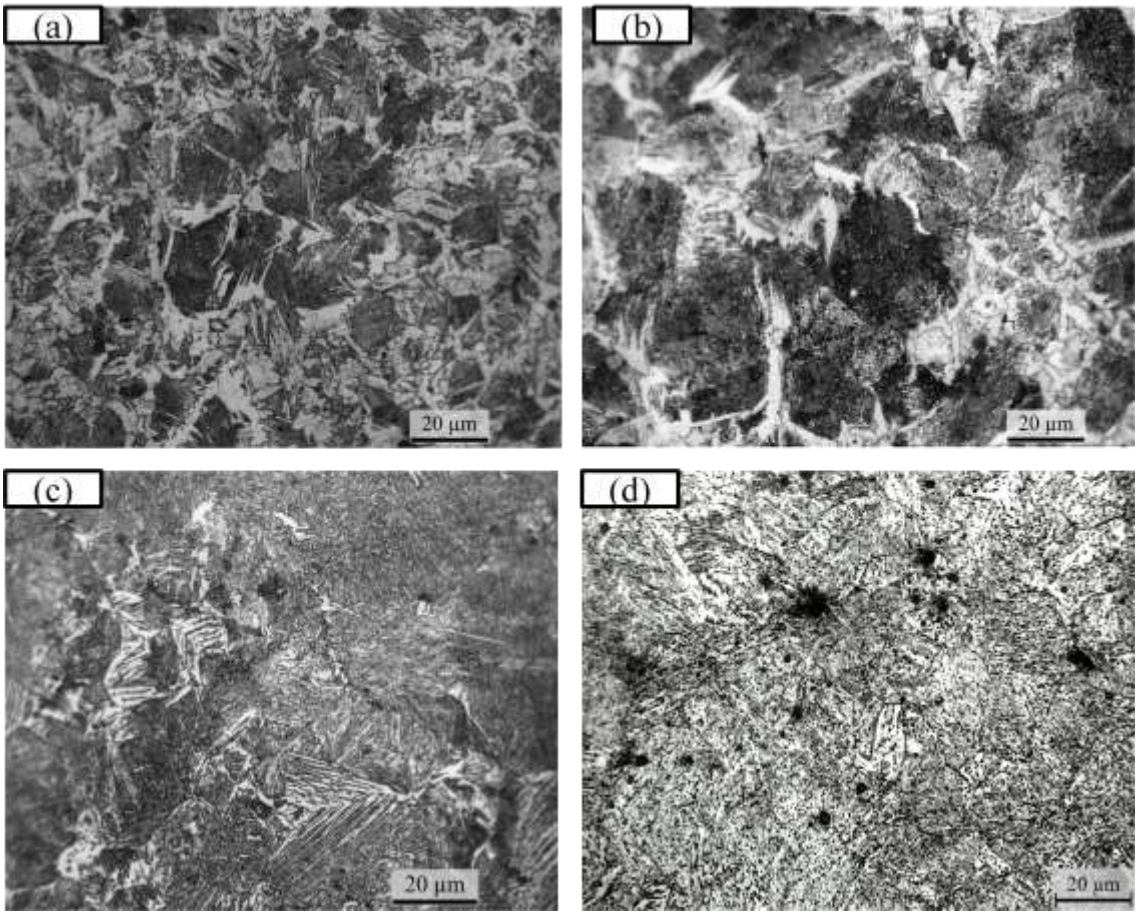

Fig. 27: Micro structures of (a) Fe-0.7C (b) Fe-2Cu-0.7C (c) Fe-2Cu-0.7C-0.5Mo (d) Fe-2Cu-0.7C-1.5Mo in Quench plus tempered condition

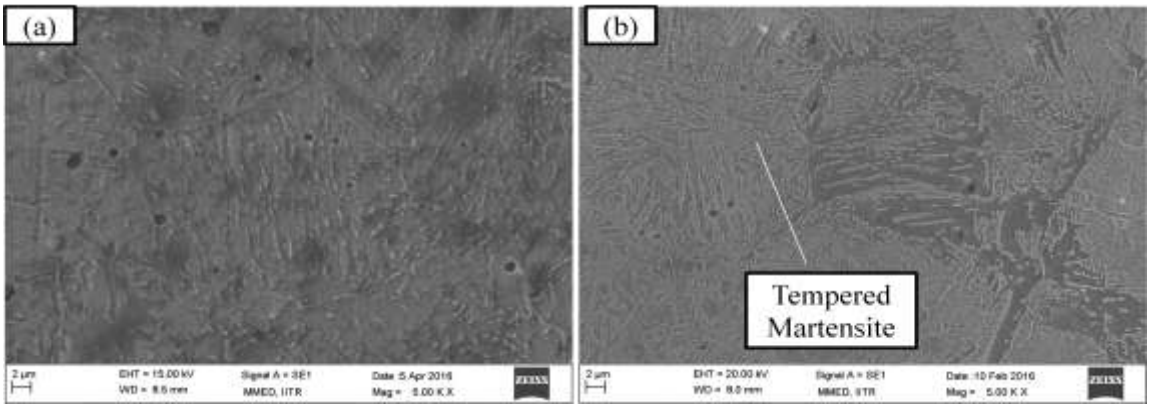

Fig. 28: SEM images of (a) Fe-2Cu-0.7C-0.5Mo (b) Fe-2Cu-0.7C-1.5Mo in quench plus tempered condition

5.5 Wear results:

5.5.1 COF variation with load and speed

Variation of coefficient of friction measured during the dry sliding tests conducted at the applied normal load of 20N, 30N, 40N with different sliding speeds of 2m/s and 3.5 m/s are shown in Fig. 29 and 30 for different compositions. The frictional force was displayed in the monitor and was noted in regular intervals. Frictional force per applied load gives us coefficient of friction (COF). Then average values are taken after each experiment and variation is plotted with respect to sliding distance.

It was noted that COF reduces as the applied load is increased. Same is noted when the sliding velocity is also increased. Surface oxidation occurred due to high temperature interface led to formation of oxides at the surface. These oxides present at the surface create less material contact which led to the decrease in COF. With further sliding of the material, surface roughness of disc reduces and the fresh metal surface revealed got oxidized due to heat of deformation which formed a protective layer at surface of disc metal. This caused less material contact and generation of wear debris consequently reducing the coefficient of friction. This situation continued with further sliding and time. Eventually, a dynamic balance was developed between formation and removal of oxide layer and COF reached a steady state.

Specimens with 1.5 wt% molybdenum under quench plus tempered condition showed the least coefficient of friction (0.37), whereas 0 wt% Cu specimens under normalized heat treated condition exhibited highest coefficient of friction (0.65). This can be seen that addition of Mo decreases the COF. This is due to the formation of bainite structure in normalised condition and tempered martensite in quench plus tempered condition. It can also be compared with the hardness values, as increase in hardness decreases the COF. Also, COF is to be lower in maximum speed and load condition. As the temperature of interface increases with increase in load, the oxide layer formed will protect the layer below it which leads to reduction in COF. Delamination of oxide film is the reason behind the reduction of COF. With addition of copper, the least COF is observed in the highest load. The sticky oxide layer formation led to decrease in COF in the alloyed steel. The same trend was observed with addition of Mo.

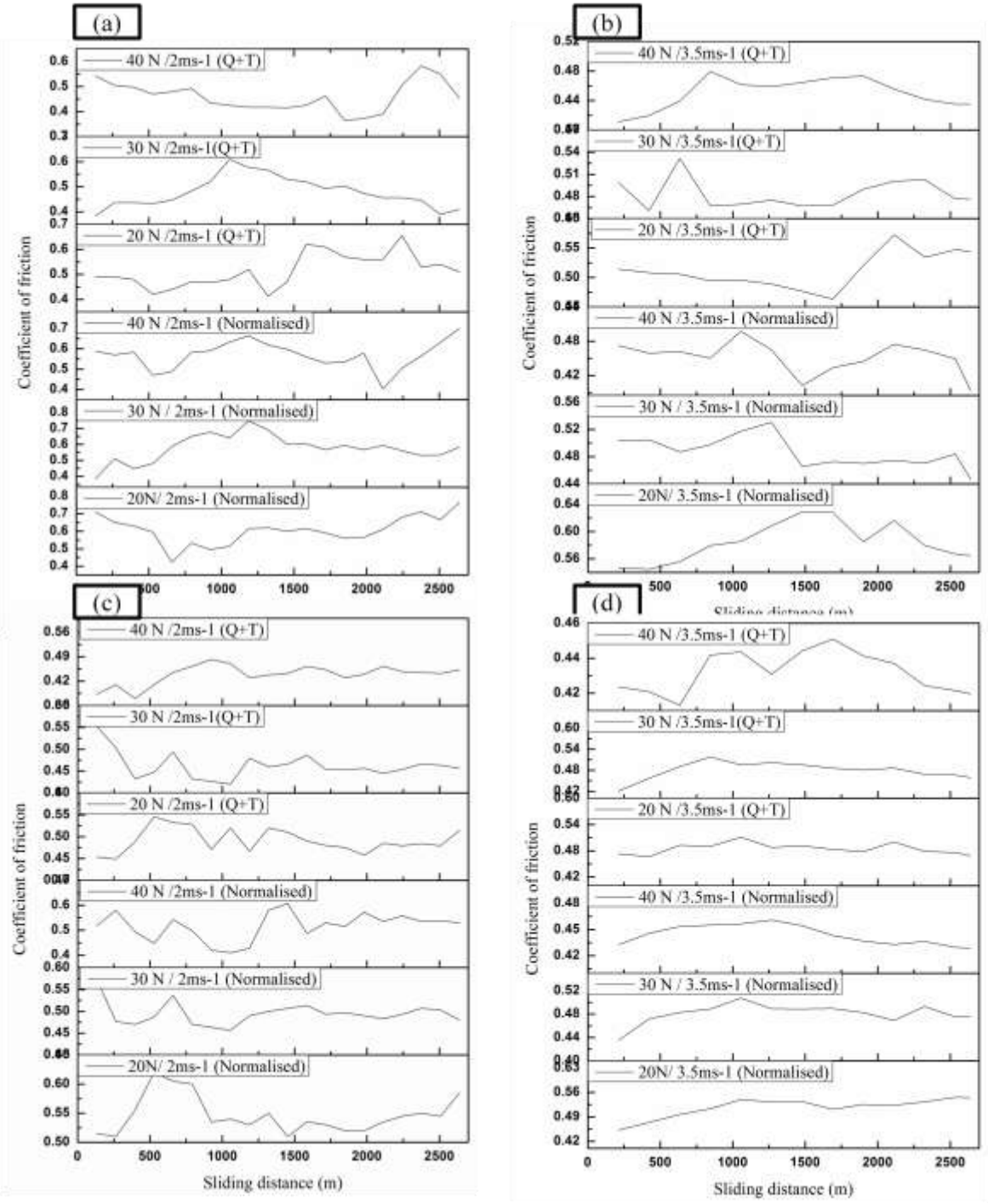

Fig. 29: Variation of coefficient of friction with respect to sliding distance of (a) Fe-0.7C ($2ms^{-1}$) (b) Fe-0.7C ($3.5ms^{-1}$) (c) Fe-2Cu-0.7C ($2ms^{-1}$) (d) Fe-2Cu-0.7C ($3.5ms^{-1}$)

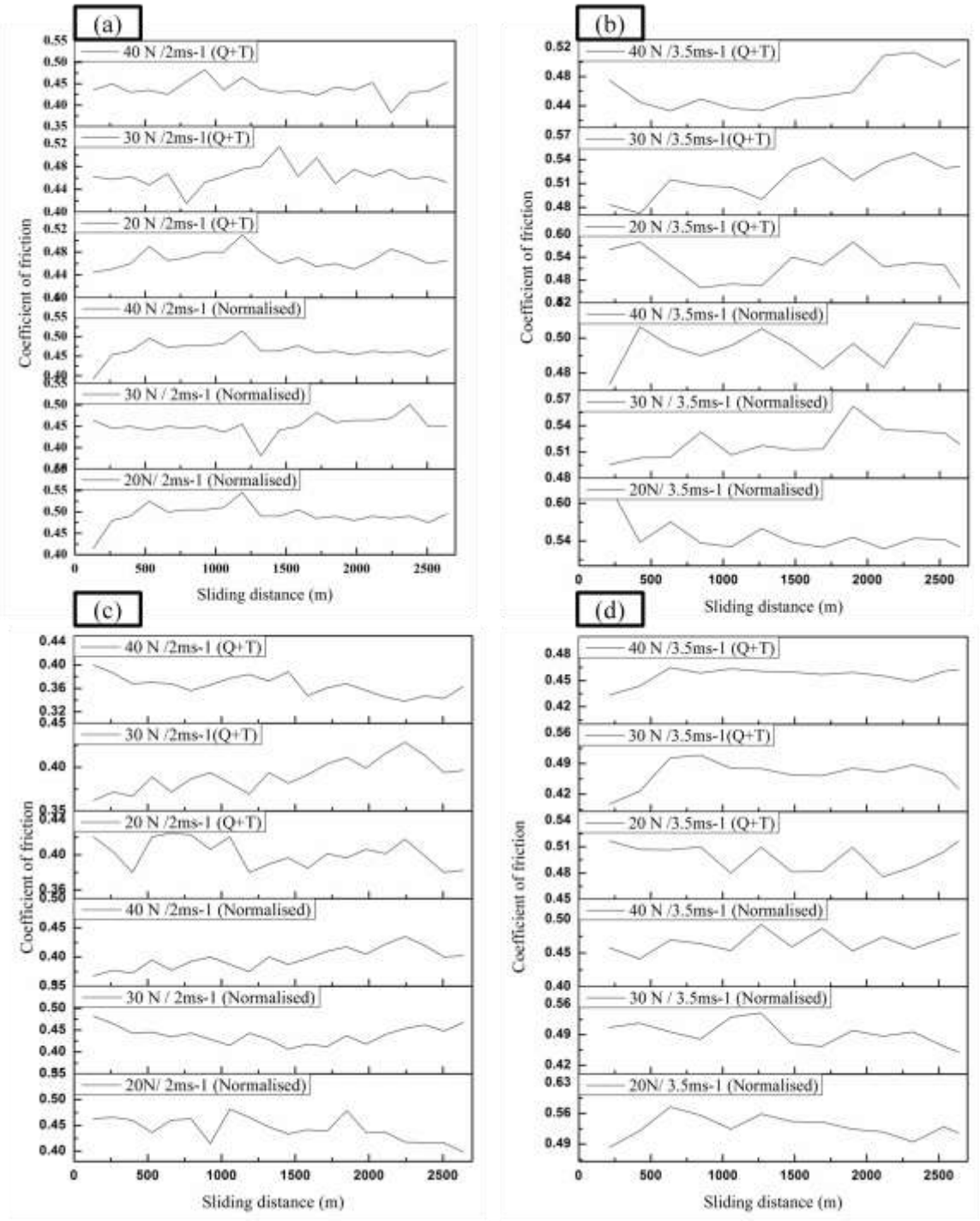

Fig. 30: Variation of coefficient of friction with respect to sliding distance of (a) Fe-2Cu-0.7C-0.5Mo ($2ms^{-1}$) (b) Fe-2Cu-0.7C-0.5Mo ($3.5ms^{-1}$) (c)Fe-2Cu-0.7C-1.5Mo($2ms^{-1}$) (d) Fe-2Cu-0.7C-1.5Mo ($3.5ms^{-1}$)

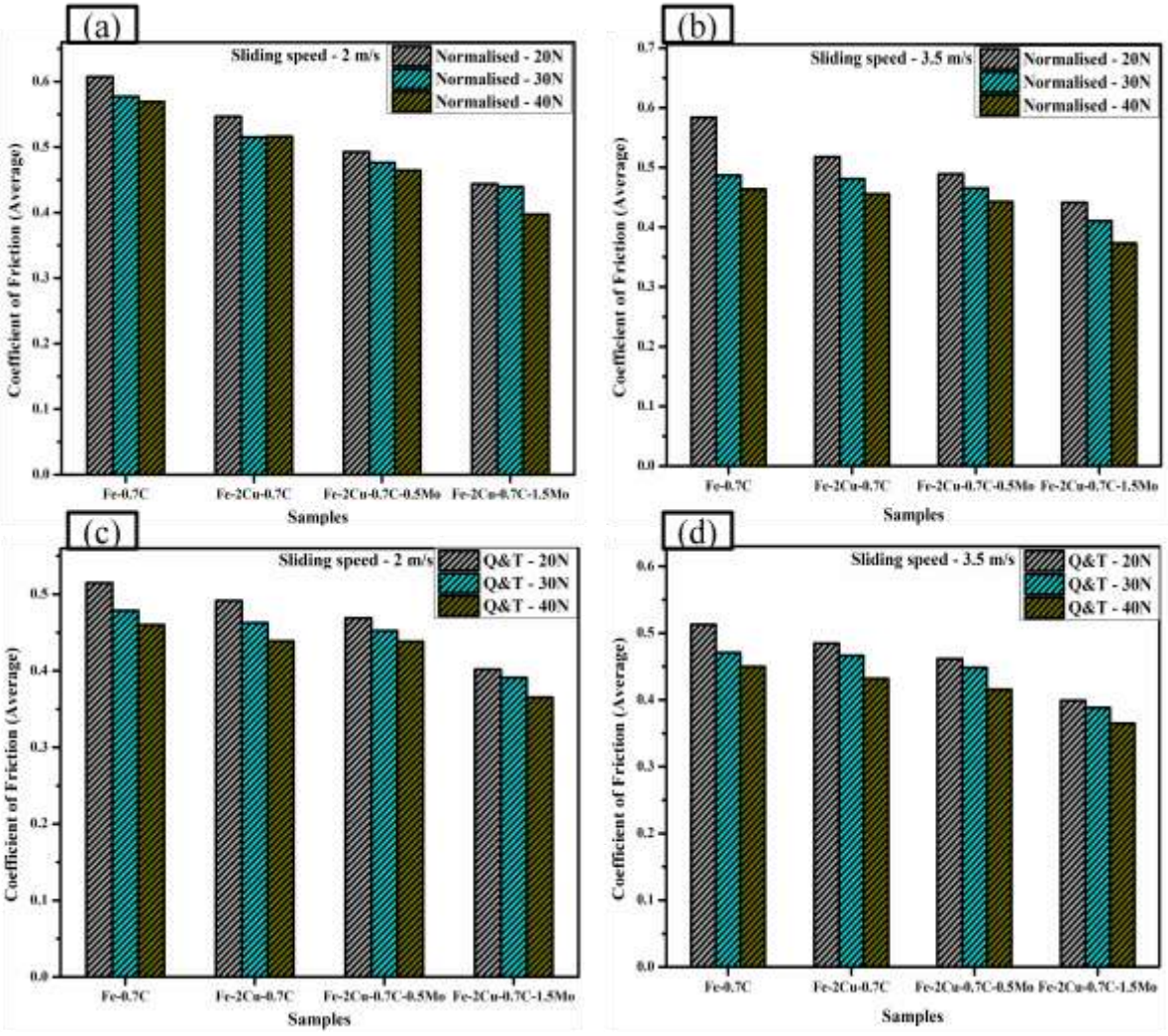

Fig. 31: Average Coefficient of friction (COF) of samples at (a) constant speed (2 m/s) normalised (b) constant speed (3.5 m/s) normalised (c) constant speed (2m/s) Q+T (d) constant speed (3.5 m/s) Q+T

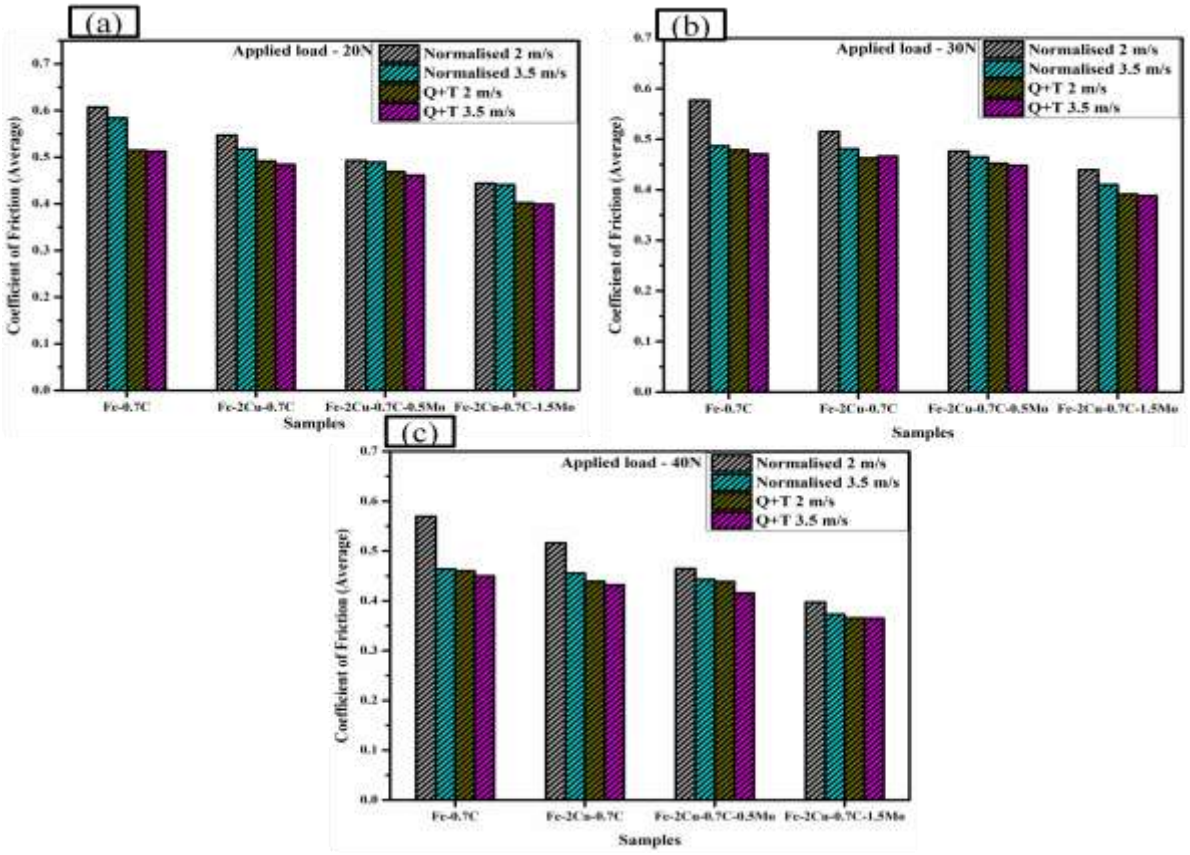

Fig. 32: Average Coefficient of friction (COF) of samples at (a) constant load (20N) (b) constant load (30N) (c) constant load (40N) condition

Fig.31 (a) shows the variation of COF under constant sliding speed of 2ms^{-1} of alloy system under normalised condition. It can be seen that addition of load applied decreases the COF for all the samples. This is due to the change in the shear rate which can influence the mechanical properties of the mating materials. In addition to this, the effect of Mo addition also influences the COF. Due to addition of Mo the COF was found to decrease. This is due to the formation of homogenous bainitic structure which is formed due to addition of Mo. The same phenomenon is observed under same constant sliding speed (2 ms^{-1}) under quench plus tempered condition. But it is noted that COF value got reduced in Q+T condition compared to normalized condition. Tempered martensite formation which led to increase in hardness led to decrease in COF. The same effect can be studied in the constant sliding speed of 3.5 ms^{-1}.

Fig.32 (a) shows the variation of COF under constant applied load of 20N and variation of sliding speeds and heat treatment condition. When speed gets increased in normalised condition the coefficient of friction decreases due to the change in shear rate.

5.5.2 Weight loss versus load and speed

Both wear volume and wear rate showed similar trend. The highest wear rate was observed in the base material (plain carbon steel) and the lowest wear rate was observed in addition of 1.5%Mo in quench plus tempered condition. In normalised condition, low hardness and soft ferrite-pearlite structure in plain carbon steel supports the high wear rate and it is having low resistance to wear. On the other hand the presence of bainite in addition of molybdenum showed better resistance to wear and hence, less wear rate. The wear rate of different samples under different conditions is shown in Fig.33 and Fig.34 below. With increase in applied load, wear rate was found to decrease. But with increase in sliding velocity, the wear rate found to increase. The weight loss increases with increase in load as well as increase in speed. The weight losses of different samples under different conditions are shown in table below.

Table 5. Weight loss of samples under normalised condition

S No	**Condition**	**Weight(g)**			
		Fe-0.7C	**Fe-2Cu-0.7C**	**Fe-2Cu-0.7C-0.5Mo**	**Fe-2Cu-0.7C-1.5Mo**
1	20N/2ms^{-1}	0.036	0.035	0.029	0.027
2	30N/2ms^{-1}	0.039	0.038	0.035	0.029
3	40N/2ms^{-1}	0.042	0.039	0.035	0.034
4	20N/3.5ms^{-1}	0.045	0.042	0.038	0.032
5	30N/3.5ms^{-1}	0.049	0.047	0.038	0.034
6	40N/3.5ms^{-1}	0.057	0.055	0.052	0.042

Table 6. Weight loss of samples under Q+T condition

S No	Condition	Weight(g)			
		Fe-0.7C	Fe-2Cu-0.7C	Fe-2Cu-0.7C-0.5Mo	Fe-2Cu-0.7C-1.5Mo
1	20N/2ms^{-1}	0.030	0.028	0.025	0.022
2	30N/2ms^{-1}	0.032	0.031	0.025	0.024
3	40N/2ms^{-1}	0.039	0.038	0.032	0.027
4	20N/3.5ms^{-1}	0.032	0.029	0.026	0.023
5	30N/3.5ms^{-1}	0.039	0.034	0.029	0.027
6	40N/3.5ms^{-1}	0.045	0.042	0.040	0.032

Weight loss increases with increase in load is the general trend observed in alloy steels. Delamination of oxide layer at the contact surface is the main reason behind this which increases the wear rates. Weight loss is higher with increase in load in case of plain carbon steels compared to other alloying additions. Same trend is observed in the case of increase in speed. Soft phase of ferrite-pearlite accounts for appreciable weight loss during wear. At higher speeds and loads, the increase in temperature which led to formation of oxide layer led to increase in wear.

Addition of copper in plain carbon steel led to slight increase in weight loss compared to plain carbon steel. Delamination wear mechanism is the reason behind the loss. As copper is oxide forming element, due to increase in temperature oxidation reaction is enhanced forming a sticky layer of oxide at the wear surface which led to decrease in wear compared to plain carbon steel. Also, the free carbon embedded around the grain boundaries led to formation of sticky layer of oxide. The highest weight loss is observed in 40N and 3.5 ms^{-1}. The delamination effect may be due to enhanced interfacial friction and high energy at the interface.

Addition of Mo as an alloying element led to less weight loss compared to plain carbon and copper added steels. Weight loss increases with increase in load as well as speed. The weight loss is less as compared to plain carbon steels. As Mo is known carbide forming

element, the carbides formed occupies the grain boundary region and strengthens it. This enhances the wear resistance of steels.

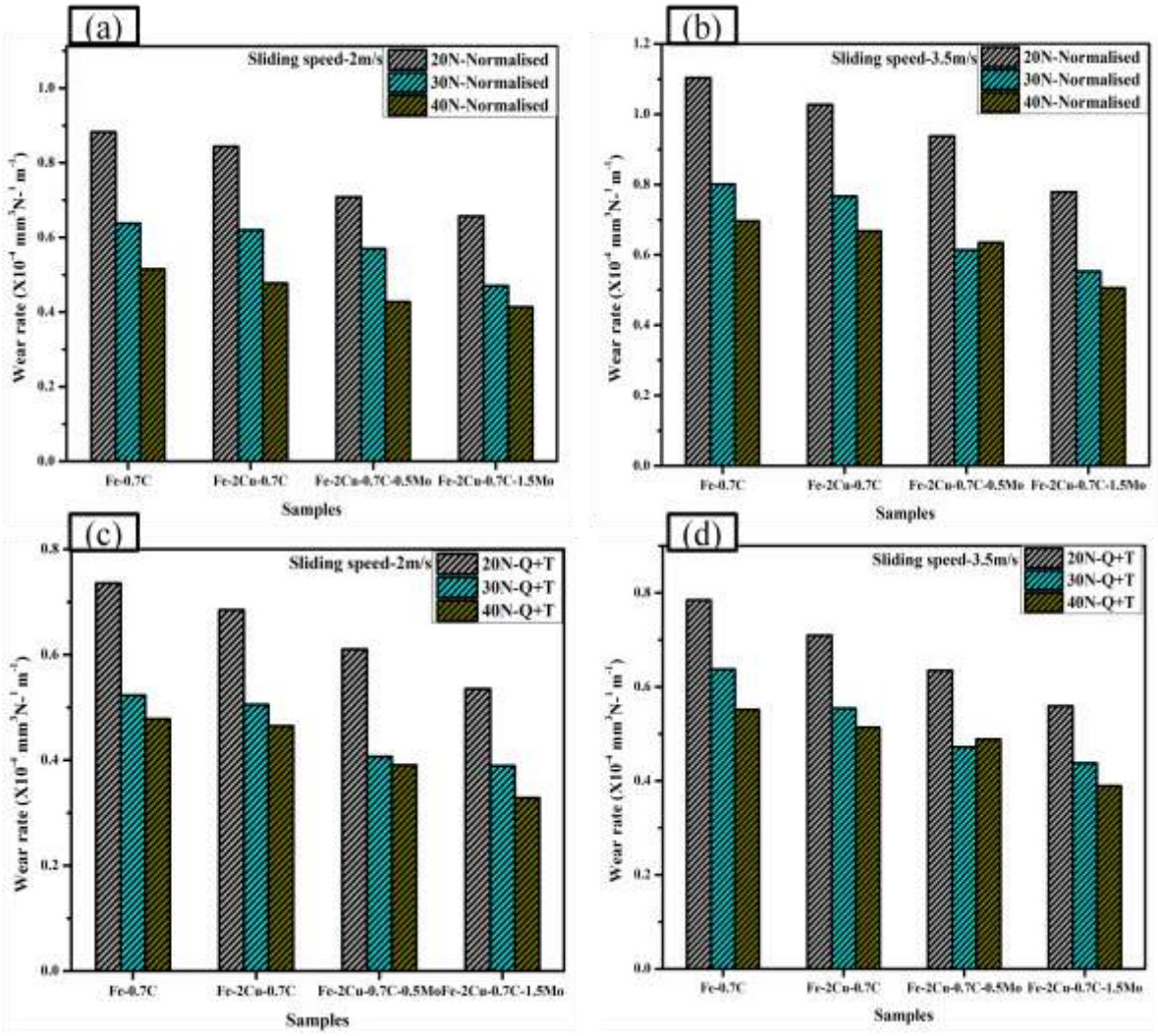

Fig. 33: Wear rate of samples at (a) constant speed (2 m/s) normalised (b) constant speed 3.5 m/s) normalised (c) constant speed (2 m/s) Q+T and (d) constant speed (3.5 m/s) Q+T

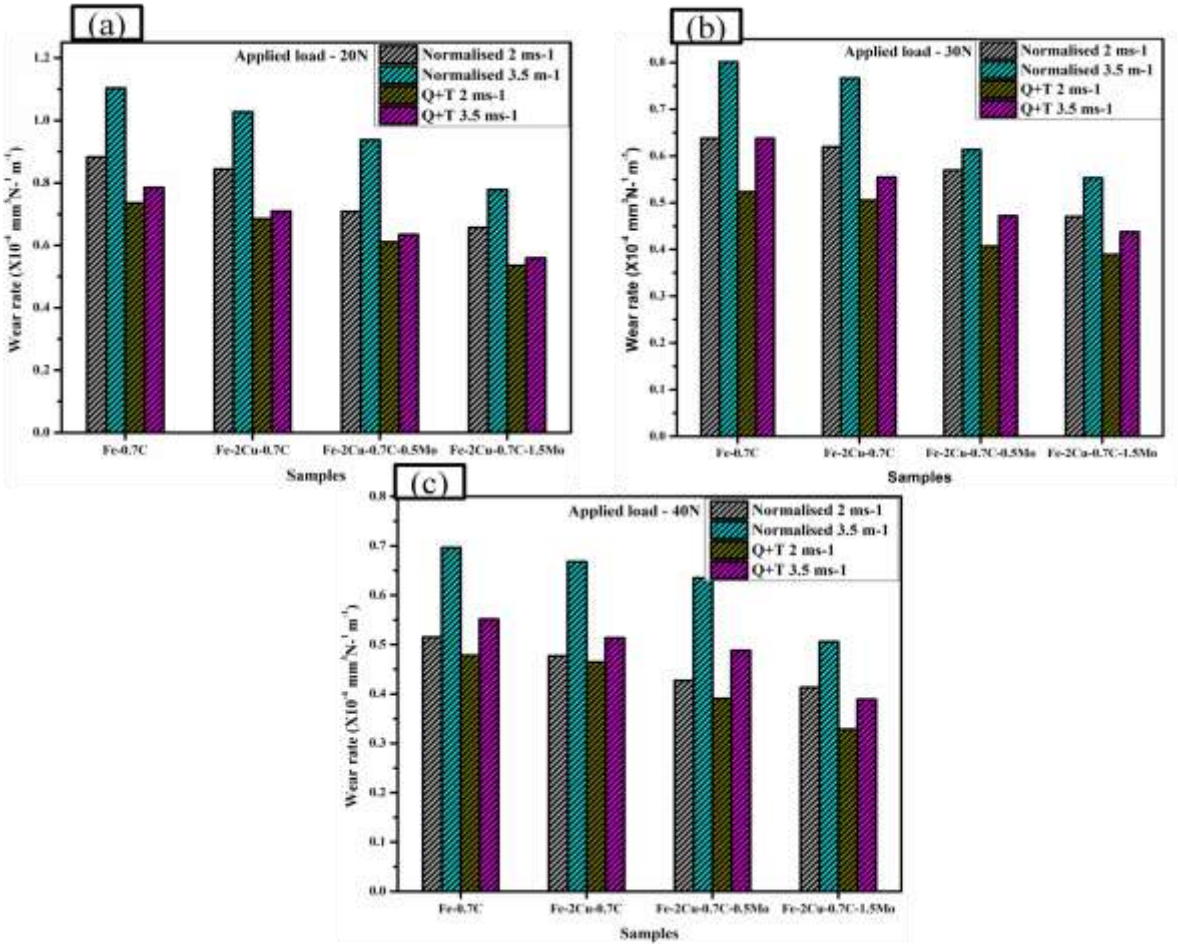

Fig. 34: Wear rate of samples at (a) constant load (20N) (b) constant load (30N) (c) constant load (40N) condition respectively

5.5.3 Microstructures

SEM images of alloy system under quench plus tempered condition under 40N/2ms^{-1} is shown in Fig.32 below. The worn surfaces were characterized by the presence of fine grooves parallel to the sliding direction and flake-like fragments, typical of delamination wear. During the sliding wear, friction forces cause deformation of the metal surface which in turn plastically shears the surface in the sliding direction. As the ductility of Fe-0.7C and Fe-2Cu-0.7C is relatively high due to soft ferritic–pearlitic structure, continuous sliding causes the accumulation of plastically sheared surface. This results in nucleation of crack that grows with sliding by shearing-fracture and finally delaminate the surface layer in form of flakes like debris. Apart from delamination, the worn surface also exhibits parallel lines in the direction of sliding that were formed due to abrasion by the wear debris which increases the wear rate. Because of both delamination and abrasion 0 wt% Cu alloy is subjected to higher weight loss. The bright particle observed in the image could be the wear debris trapped within the pores that may have been created by Cu dissolution. Sticking of wear debris on the sample surface also contributed to abrasion wear. During sliding wear, due to higher loads and speeds the temperature at the interface causes the oxidation present in the steel. Further wear is prevented due to the formation of oxides formed at the interface.

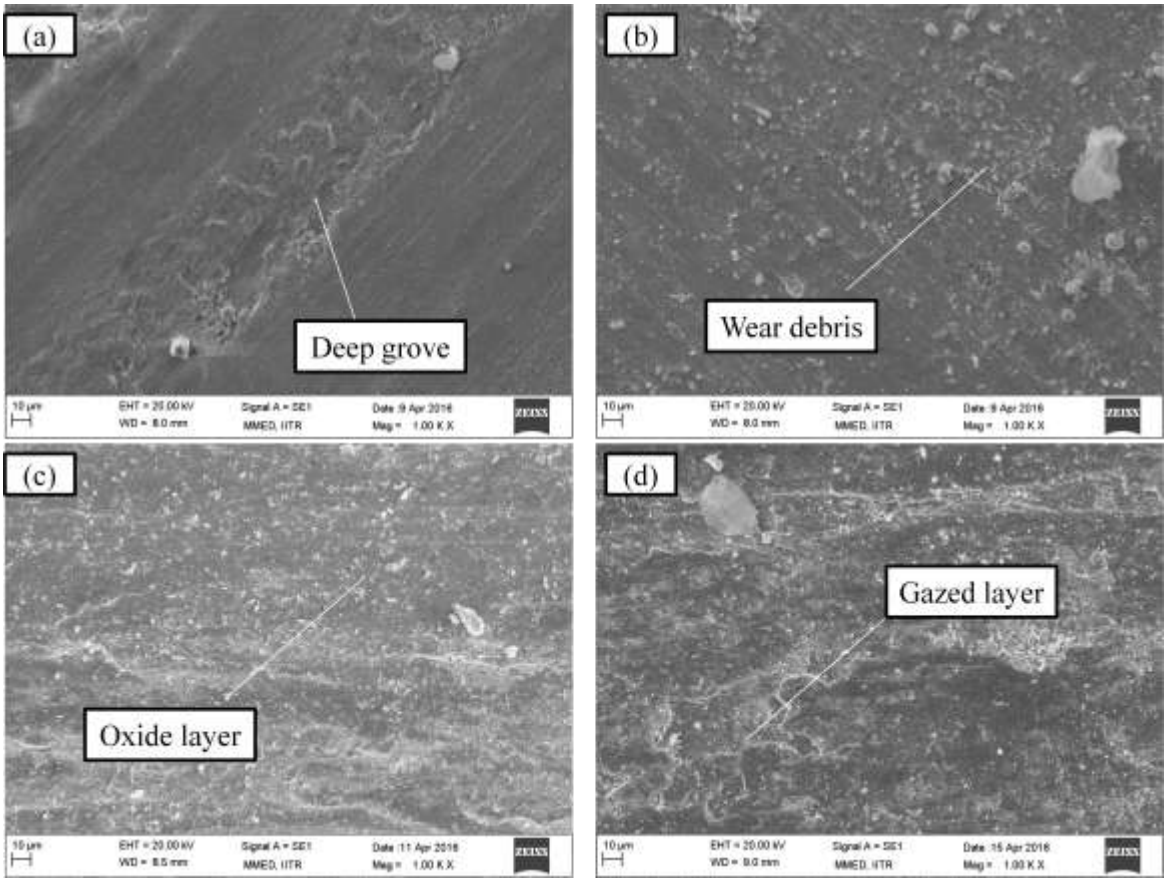

Fig. 35: SEM images of (a) Fe-0.7C (b) Fe-2Cu-0.7C (c) Fe-2Cu-0.7C-0.5Mo (d) Fe-2Cu-0.7C-1.5Mo normalised wear samples at 40N/2m/s.

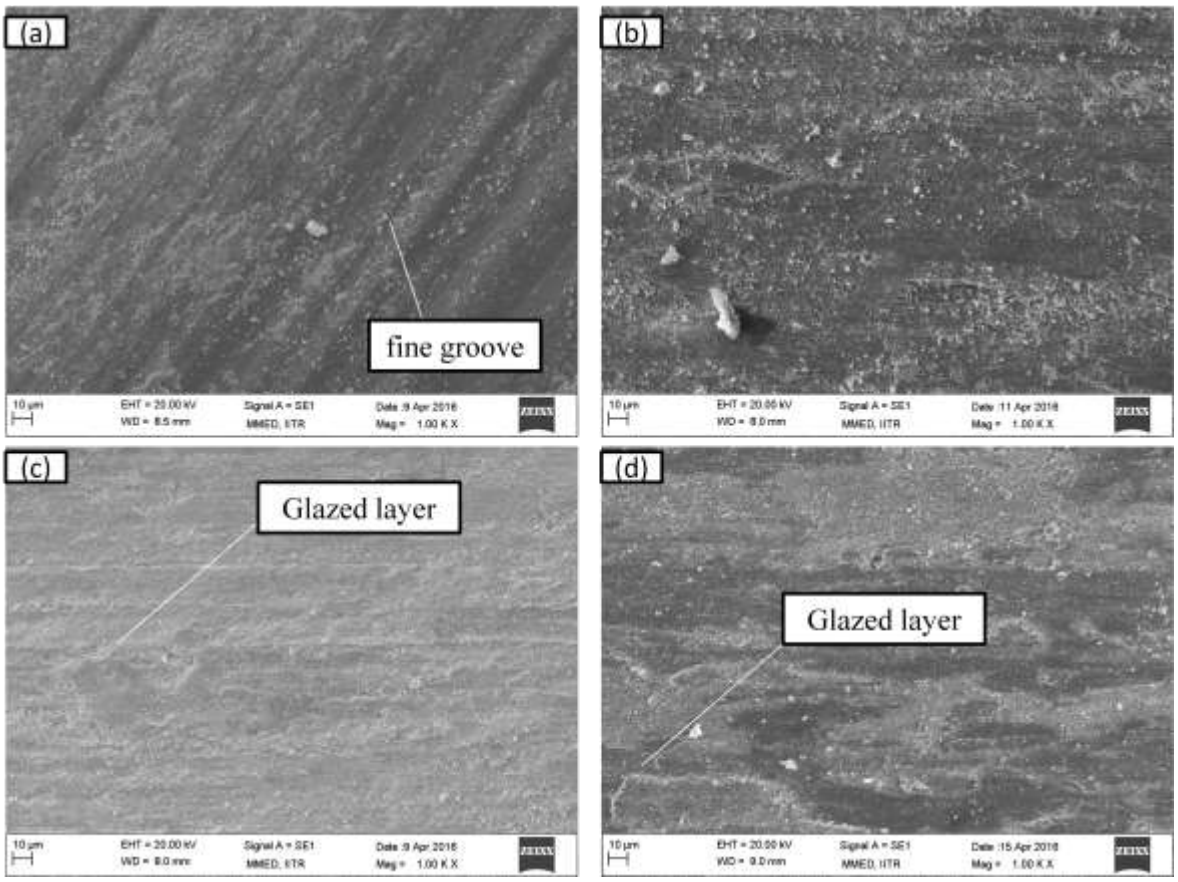

Fig. 36: SEM images of (a) Fe-0.7C (b) Fe-2Cu-0.7C (c) Fe-2Cu-0.7C-0.5Mo (d) Fe-2Cu-0.7C-1.5Mo quench plus tempered wear samples at 40N/2m/s.

The analysis of SEM images provides insight into the dominating wear mechanism prevailing under different heat treatment conditions. Mo alloyed steels are subjected to lesser wear loss compared to plain copper and carbon steels. In 1.5 wt% Mo steels glazed layer is clearly evident. Formation of glazed layer is more visible in 1.5 wt% Mo steels compared to 0.5wt% Mo steels and is reason for lesser wear rate. A continuous surface oxides layer which could be FeO is mechanically stable and delineates oxidative wear as dominating mechanism in 1.5 wt% Mo samples.

Presence of oxide layer in all images showed oxidative wear mechanism in both the heat treatment conditions. However, presence of some wear debris and detachment of oxide

layer also manifested abrasion as well as delamination wear especially in quench plus tempered specimens as dominating wear mechanism.

Since tempering improves strength and toughness due to tempered martensitic structure, improved wear resistance was observed in the quench plus tempered condition as compared to normalised condition. The SEM image of quenched condition exhibited small discontinuous fragments of oxides layer and flakes on the worn surface.

The results of tribological behavior for 1.5 wt% Mo alloys under different heat treatment conditions and varying Mo contents in normalised conditions demonstrate that the wear is a complex and complicated mechanism in Fe-Cu-C-Mo alloyed steel. One universal mechanism is not sufficed to explain it fully. In fact, it depends on several factors including hardness, microstructure, porosity, strength, ductility and toughness as well as wear conditions. The results indicate that with improved mechanical properties such as strength, toughness and hardness better wear resistance may be achieved. Therefore, from the results of mechanical and tribological study it may be concluded that the quench plus tempered heat treatment is beneficial for improved mechanical as well as tribological properties and is recommended for high performance application.

6. SUMMARY

- The forged alloys exhibited a porosity level of < 1.95% as copper rapidly flows into the pore network and diffuses into the iron forming a solid solution.
- During normalizing heat treatment, pearlite and ferrite phases are seen in Fe-0.7C and Fe-2Cu-0.7C system. But addition of molybdenum gives a complex structure which is bainite as per literature.
- Hardness was found to increase with Mo addition for normalised and quench plus tempered conditions.
- Tensile properties were significantly influenced by the addition of Mo as well as the heat treatment conditions. Highest strength was observed in 1.5 wt% Mo in quench plus tempered condition and was found to be around 1280MPa.
- The wear behavior was influenced by both Mo addition and heat treatment conditions.
- Addition of Mo promotes oxidative wear as dominating wear mechanism and forms an oxide layer which therefore, protects the sliding surface from further wear. On the other hand 0 wt% Cu (Fe-0.7C) and 0 wt% Mo (Fe-2Cu-0.7C) exhibited delamination and abrasion as dominating wear mechanism and consequently showed lower wear resistance.
- In normalised condition addition of Mo causes transition of wear mechanism from delamination and abrasion in 0 wt% Mo specimens to oxidative wear in 1.5 wt% Mo specimens.
- Highest wear rate was exhibited in plain carbon steel under normalised condition whereas lowest wear rate was observed in 1.5 wt% Mo under quench plus tempered condition.

7. SCOPE OF FUTURE WORK

- Fatigue and impact properties can be investigated for high stressed and variable loading conditions.
- Secondary hardening effect with Mo addition at different tempering temperatures can be carried out for elaborate studies of formation of carbide.
- Machinability studies for the present alloy system can also be studied for the different heat treatment conditions.
- Generation of deformation maps of sinter-forged Fe-Cu-C-Mo alloy system and study the deformation mechanism under different conditions.
- For further enhancement of toughness and ductility, alloy additions like Mn, Ni etc. may be carried out.

8. LIST OF PUBLICATIONS

Vignesh.S, Vikram.V.Dabhade, “Dry sliding wear studies on sinter-forged Fe-Cu- C-xMo alloys”, presented at International conference on powder metallurgy & particulate materials, Pune from 18th to 20th February, 2016.

9. REFERENCES

[1]. Ramakrishnan. P, "Automotive applications of powder metallurgy", Advances in Powder Metallurgy, Properties, Processing and Applications, A volume in Woodhead Publishing Series in Metals and Surface Engineering ,2013, pp. 493–519.

[2]. Seshendra Karamchedu, "Effect of diffusion bonded Cu and Ni on sinter hardening response on Mo prealloyed PM steels" Master's thesis, Chalmers Publication Library, Department of Materials and Manufacturing Technology, Chalmers University of Technology Sweden, 2010, pp. 224-228.

[3]. Sanjay S Rathore, Milind M Salve and Vikram V. Dabhade: "Effect of Molybdenum addition on mechanical properties of Sinter-Forged Fe-Cu-C Alloys", Journal of Alloys and compounds, 2015, pp. 988-995.

[4]. Wen-Fung Wang "Effect of alloying elements and processing factors on the microstructure and hardness of sintered and induction-hardened Fe-Cu-C alloys" Material science and engineering, 2005, pp.92-97.

[5]. Michael L. Marucci and Francis G.Hanejko "Effect of Copper Alloy Addition on Dimensional Response of Sintered Fe-Cu-C" Advances in Powder Metallurgy and Particulate materials, 2014.

[6]. Hoganas HandBook, Chapter-6, Basic mechanism of sintering, No.2, 2004, pp.6-12.Höganäs AB.

[7]. Valery Marinov, *Manufacturing technology*, Kendall Hunt publishing company, 2010.

[8]. Kandavel T.K. and Chandramouli R, "Experimental investigation on the microstructure and mechanical properties of sinter forged Cu and Mo alloyed low alloy steels", International Journal of Advance Manufacturing Technology,Vol. 50, 2010, pp.53-59.

[9]. Metals handbook, Volume 14, edition 9, ASM international, 1988.

[10]. Yilmaz R., and Ekic M.R., "Microstructural and hardness characterisation of sintered low alloyed steel", Journal of Achievements in Materials and Manufacturing Engineering,Vol. 31, 2008, pp.23-28.

[11]. D.Wilbert, T.J.Lucia, F.Jose CA, C.M.Elizabeth, F.V.C.Victor, "Effect of copper on the mechanical properties of alloys formed by powder metallurgy", Mater.Des.58, 2014, pp 12-18.

[12]. Metals handbook, Volume 14, edition 9, ASM international, 1988.

[13]. Neeraj Verma, Saurabh Anand "Effect of carbon addition and sintering temperature on densification and micro-structural evolution of sinter hardened structural steels" Journal of undergraduate material research, 2006, pp. 53-60.

[14]. Wang J., Danninger H., "Dry sliding wear behavior of molybdenum alloyed sintered steels", Wear, Vol. 222, 1998, pp. 49–56.

[15]. Juan Wang, Herbert Danninger, "Dry sliding behavior of Molybdenum alloyed sintered steels", Wear 222, 1988, pp 49-56.

[16]. Bruce Lindsley, George Fillari, Thomas Murphy "Effect of composition and cooling rate on physical properties and microstructure of prealloyed steels" Hoganaes Corporation, Cinaanmison NJ, 2002,pp.202-212.

[17]. Kandavel T.K., Chandramouli R., Manoj M., Manoj B., Gupta D.K., " Influence of copper and molybdenum on dry sliding wear behaviour of sintered plain carbon steel", Materials and Design,Vol. 50, 2013, pp. 728-736.

[18]. Bernier F., Gauthier M., Plamondon P., L'Espérance G., "Copper strengthening of PM steel parts, International Journal of Powder Metallurgy, Vol.47 (6) , 2011, pp. 11-19.

[19]. Tekeli S. and Gural A., "Dry sliding wear behaviour of heat treated iron based powder metallurgy steels with 0.3% graphite + 2% Ni additions", Materials and Design, Vol.28,2007, pp. 1923-1927.

[20]. Lindskog P. and Thornblad O., "Ways to improve the strength components made from partially pre-alloyed steel powders", Powder Metallurgy International, Vol. 11(1), 1979, pp. 10-11.

[21]. Lindsley B. A. and Rutz H. G., "Effect of molybdenum content in PM steels, Advances in Powder Metallurgy& Particulate Materials, Vol.7, 2008, pp. 26-40,.

[22]. Narasimhan K.S., “Recent Advances in Ferrous Powder Metallurgy”, Advanced Performance Materials, Vol.3, 1996, pp.7-27.

[23]. Salak A. and Selecka M., “Wear behaviour of carbon and low alloyed sintered steels”, Powder Metallurgy Progress, Vol. 2 (4), 2002, pp. 231-242.

[24]. Tengzelius J., Grek S.E., Blande C.A., “Modern developments in powder metallurgy”, Vol.13, 1980, pp.159-182.

[25]. Torralba J. M., Combronero L.E.G., Ruiz J.M., “ Influence of the nature of powders on properties and microstructure of sintered Cu and Ni steels”, Powder Metalllurgy International, Vol.24(4), 1992, pp.226-228.